# Electron Momentum Spectroscopy of Norbornadiene at the Benchmark ADC(3) Level

**ARTICLE** *in* THE JOURNAL OF PHYSICAL CHEMISTRY A · SEPTEMBER 2010

Impact Factor: 2.69 · DOI: 10.1021/jp105551j · Source: PubMed



**3 AUTHORS**, INCLUDING:

Filippo Morini
Hasselt University
**18** PUBLICATIONS **114** CITATIONS
SEE PROFILE

Michael S Deleuze
Hasselt University
**132** PUBLICATIONS **2,673** CITATIONS
SEE PROFILE

# Electron Momentum Spectroscopy of Norbornadiene at the Benchmark ADC(3) Level

**Filippo Morini, Balázs Hajgató, and Michael S. Deleuze***

*Research Group of Theoretical Chemistry and Molecular Modelling, Hasselt University, Agoralaan Gebouw D, B-3590 Diepenbeek, Belgium*

*Received: June 16, 2010; Revised Manuscript Received: July 13, 2010*

An extensive study, throughout the valence region, of the electronic structure, ionization spectrum, and electron momentum distributions of norbornadiene is presented, on the ground of accurate calculations of valence one-electron and shake-up ionization energies and of the related Dyson orbitals, using one-particle Green's function (1p-GF) theory in conjunction with the so-called third-order algebraic diagrammatic construction scheme [ADC(3)]. Comparison is made with results obtained from standard (B3LYP) Kohn−Sham orbitals and measurements employing electron momentum spectroscopy, taking into account the contamination of inner- and outer-valence spectral bands by numerous shake-up states. Four relatively intense shake-up lines at 12.1, 16.4, 17.6, and 17.8 eV are found to yield recognizable spectral fingerprints in the EMS experiments. Valence bands at electron binding energies larger than 20 eV are subject to a complete breakdown of the orbital picture of ionization.

## I. Introduction

The electronic structure of bicyclo[2,2,1]heptadiene, a formally nonconjugated diene and highly strained cage compound most commonly referred to as norbornadiene (Figure 1), has been a few years ago subject to rather contradictory experimental studies[1−3] employing electron momentum spectroscopy (EMS).[4,5] By virtue of a combination of the principles of scattering and ionization experiments, this powerful orbital imaging technique enables experimental reconstructions of spherically averaged one-electron transition momentum distributions corresponding to specific ionization channels, according to an angular analysis of ionization intensities in binary (e, 2e) electron impact ionization experiments ($M + e^- \rightarrow M^+ + 2e^-$) at high kinetic energies and under a nonplanar symmetric kinematical setup.

Interest in norbornadiene stems from numerous photoelectron[6−8] and theoretical[9−16] studies of through-space and through-bond interactions[17−19] between the ethylene $\pi$-orbitals ($\pi_1$, $\pi_2$) associated with the two double bonds. Of relevance also is a study of the electronic structure of norbornadiene using Penning ionization electron spectroscopy by Ohno et al.[20] The consensus that emerged over the years is that in this compound, through-space interactions dominate through-bond interactions and lead to a destabilization of the out-of-phase ($\pi^- = \pi_1 - \pi_2$) with respect to the in-phase ($\pi^+ = \pi_1 + \pi_2$) combinations of the $\pi$-ethylene orbitals. By affording experimental reconstructions in momentum space of orbital densities, according to the basic one-electron picture of ionization, the available EMS studies[1−3] rather clearly confirm that, in contrast for instance with 1,4-cyclohexadiene,[1] the $\pi^-$ ($5b_2$) and $\pi^+$ ($7a_1$) one-electron ionization levels coincide with the highest occupied molecular orbital (HOMO) and next-to-highest occupied molecular orbital (NHOMO).

However, a most puzzling issue which in our opinion needs to be readdressed are rather strong and sharp turn-ups of the electron momentum distributions recorded for these two levels by Mackenzie-Ross and his co-workers at vanishing electron momenta ($p < 0.1$ au, with 1 au = 1 $bohr^{-1}$),[2,3] which are not observable in the EMS measurements by Takahashi et al.,[1] possibly due to a too low resolution on electron momenta, and which have been tentatively ascribed[3] to electron correlation effects, according to simulations employing a variety of Kohn−Sham orbitals and some analogy with results obtained from other structurally similar cage compounds (amantadine, urotropine[21]). Mackenzie-Ross et al. extended their investigation of the electronic structure of norbornadiene down to the bottom of the inner-valence region,[3] on the sole ground of a comparison of experimentally inferred electron momentum distributions at specific binding energies with simulations drawn from spherically averaging resolution-folded structure factors derived from a variety of Kohn−Sham orbitals. In their study, they apparently did not exploit early (outer valence) Green's function calculations by von Niessen and Diercksen,[13] or Galasso,[15] in conjunction with rather modest basis sets. Severe breakdowns of the one-electron picture of ionization, in the form of a dispersion of the ionization intensity over broad and dense sets of numerous shake-up satellites,[22,23] were rather implicitly and very crudely accounted for by an ad hoc rescaling of the simulated innermost electron momentum distributions.

The purpose of the present work is to reassign the available (e, 2e) ionization spectra of norbornadiene and the correspondingly inferred electron momentum distributions, according to more robust calculations of the valence one-electron and shake-up ionization energies and of the corresponding Dyson orbitals,[24] using the well-established third-order algebraic diagrammatic construction [ADC(3)] scheme[25] derived within the framework of one-particle Green's function theory (also referred to as electron propagator theory[26]). The main motivations for the present work stem from recent studies[27] at the same level of the ionization spectra of various dione cage compounds and

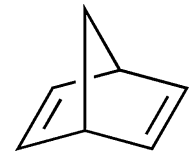

**Figure 1.** Molecular structure of norbornadiene.

* Corresponding author. E-mail: michael.deleuze@uhasselt.be.

10.1021/jp105551j 
Published on Web 08/06/2010

most convincing demonstrations therein that it is absolutely impossible to reliably interpret highly congested (e, 2e) ionization spectra by resorting only to Kohn−Sham orbital energies and to the related electron momentum distributions. Also, recent studies by our group[28] employing ADC(3) Dyson orbitals upon 1,3-butadiene, thiophene, and cyclopentene show that intensity redistributions due to shake-up transitions have to be taken into account for physically meaningful simulations of the experimentally inferred (e, 2e) momentum profiles. Besides the contamination of spectral bands by shake-up lines, it is certainly worth recalling here that EMS experiments are subject to many complications,[29] such as thermally induced nuclear motions (including conformational rearrangements) in the electronic ground state,[30] ultrafast nuclear dynamics,[31] or Jahn−Teller effects[32] in the final cationic state, as well as postcollision and distorted wave effects.[33]

## II. Computational Details

All computations that are presented in this work have been carried out upon a geometry that was optimized under the constraint of the $C_{2v}$ symmetry point group using density functional theory (DFT[34]), in conjunction with the standard hybrid gradient corrected Becke−3-parameters−Lee−Yang−Parr (B3LYP) functional[35] and using Dunning's triple-$\zeta$ polarized valence (TZVP) basis set,[36] in straightforward analogy with former theoretical studies of EMS measurements of many other cage compounds (see ref 27 and references therein, as well as ref 37).

The valence one-electron and shake-up ionization spectrum of norbornadiene has been calculated by solving at the 1p-GF/ADC(3) level a CI-like secular matrix equation $\mathbf{HX} = \mathbf{XE}$ (with $\mathbf{XX}^{\dagger} = \mathbf{1}$) cast over primary one-hole (1h) and singly excited two-hole-one-particle (*2h-1p*) shake-*up* cationic states, as well as one-particle (1p) and singly excited two-particle-one-hole (*2h-1p*) shake-*on* anionic states, by comparison[25] with a through-third- and through-fourth-order diagrammatic analysis of the dynamic and static self-energies embodied in the standard Dyson expansion of the 1p-GF (see, e.g., Figure 1 in ref 25e for a complete diagrammatic overview of all involved self-energy terms). The ADC(3) scheme is known to enable calculations of one-electron ionization energies at a level of accuracy (∼0.2 eV) comparable to that reached with the multireference single−double configuration-interaction (MR-SDCI) scheme (see ref 38 and references therein), with the key advantages of size consistency and of a greater compactness of the secular matrix to diagonalize. Singly excited *2h-1p* (*2p-1h*) states are correspondingly described through first-order only, which implies lower accuracies on shake-up ionization energies, in particular those corresponding to lines with lower intensity, i.e., 1h character. In both cases, the Feynman−Dyson transition amplitudes ($x_i^{(n)}$) needed to expand the related Dyson orbitals and spectroscopic strengths can be identified[24,28] with the 1h + 1p components of the associated eigenvectors ($X_{\mathrm{in}}$).

The ADC(3) computations have been carried out using the original package of programs interfaced to GAMESS,[39] using the molecular $C_{2v}$ symmetry point group for limiting the dimension of the secular matrices to diagonalize, under the assumption of frozen core electrons, and resorting to the band Lanczos diagonalization approach[40] for projecting in a first step the 2p-1h shake-on states associated with the electron affinity blocks of the secular matrix to diagonalize onto a pseudoelectron attachment spectrum, prior to the final diagonalization of the **H** matrix, this time by means of the block-Davidson approach.[41] All eigenstates with a pole strength larger than or equal to 0.005 have been recovered up to electron binding energies of 30 eV. At the SCF level, the requested convergence on the elements of the one-electron density matrix was set equal to $10^{-10}$.

The sensitivity of ADC(3) results for shake-up lines at outer-valence ionization energies upon the quality of the basis set has been recently questioned in an analysis of EMS experiments upon pyrimidine.[42] In the present work, we shall therefore comparatively assess ADC(3) calculations performed using three basis sets of improving quality: the standard Pople's 6-31G basis set,[43] Dunning's correlation consistent polarized valence basis set of double-$\zeta$ quality (cc-pVDZ[44]) and the standard Dunning's double-$\zeta$ basis set with polarization and diffuse functions (DZP+[45]). These three basis sets incorporate on total 79, 145, and 181 atomic functions in the calculations.

Theoretical ADC(3) ionization spectra are presented in the sequel in spike and convoluted forms, using as convolution function a Voigt profile combining Gaussian and a Lorentzian functions with equal weight and a constant full width at half-maximum (fwhm) parameter of 0.6 or 0.9 eV. These parameters and line shapes have been selected to enable comparisons with available ultraviolet (He I, He II) photoelectron spectroscopic (UPS) or EMS measurements, respectively, taking roughly into account in these simulations the experimental energy resolution (∼0.55 eV) in the EMS measurements by Mackenzie-Ross et al.,[2,3] as well as the broadening of lines due to the limited lifetime of ionized states (natural line width) and vibronic coupling interactions (vibrational broadening). In these simulations, line intensities have been scaled according to the computed spectroscopic strengths ($\Gamma_n$) or (e, 2e) cross sections, respectively. For the sake of more accurate insights into the computed ionization energies, comparison will be made with larger scale calculations employing the outer-valence Green's function (OVGF) approach.[26c−f]

In line with the usual prescriptions for analyzing EMS experiments,[1−5,28−32] (e, 2e) electron momentum distributions have been simulated according to the Born (sudden), binary encounter, and plane wave impulse approximations for a standard (e, 2e) noncoplanar symmetric kinematical setup and at the electron impact energies that Takahashi et al.[1] and Mackenzie-Ross et al.[2,3] considered in their experimental investigations. Three levels of approximations for the involved electronic structure factors have been considered, namely, the target Hartree−Fock approximation (THFA[46]), which is strictly equivalent to a description of ionization events at the level of Koopmans's theorem (neither electronic correlation nor relaxation are accounted for); the target Kohn−Sham approximation (TKSA[47]), which amounts to considering one-electron removals from Kohn−Sham orbitals in correlated DFT electronic wave functions, and the so-called target-Dyson ADC(3) approximation, therefore using ADC(3) Dyson orbitals[28] for computing (e, 2e) ionization intensities from transition moments that explicitly account for electronic correlation in the ground state, as well as electronic relaxation and configuration interactions in the final state. The interested reader is referred to recent theoretical analyses using ADC(3) Dyson orbitals[28b,c,48] by our group at Hasselt University (Belgium) of various high-resolution EMS experiments at Tsinghua University (Beijing, China), which all very quantitatively confirm the physical relevance of the latter target approximation in studies of (e, 2e) ionization processes at standard electron binding energies (0−25 eV), with respect to both the experimentally obtained ionization energies and related transition moments. The B3LYP Kohn−Sham momentum distributions have been computed in conjunction with Dunning's correlation consistent polarized valence basis

sets of double and triple-ζ quality (cc-pVDZ, cc-pVTZ), as well as the cc-pVTZ basis set augmented by a set of s, p, d, and f diffuse functions on carbons and s, p, and d diffuse functions on hydrogens (aug-cc-pVTZ basis set[49]), incorporating a total of 145, 365, and 585 atomic functions in the calculations, respectively.

Spherically averaged orbital momentum distributions have been generated from the output of 1p-GF/ADC(3) or DFT calculations using the MOMAP program by Brion and coworkers[50] and homemade interfaces. In line with the characteristics of the (e, 2e) spectrometer that was employed at Flinders University (Adelaide, Australia), our calculations of momentum distributions and of spherically averaged (e, 2e) cross sections also account for a limited resolution of $\Delta\phi = \pm 1.2°$ and $\Delta\theta = \pm 0.60°$,[2,3,51] at an impact energy of 1.5 keV. The results of the EMS experiments by Takashashi et al. on norbornadiene have been simulated by assuming similar angular resolutions but at an impact energy of 0.8 keV. In the present work, the limited resolution in momentum has been accounted for by means of a procedure employing Monte Carlo simulations.[52,53] Results obtained with this procedure were found to be virtually identical with momentum distributions that have been simulated using the Gaussian weighted planar grid approach[53] for resolution folding in momentum space.

For the sequel, it will be most useful to note that all HF and DFT calculations described in the present work have been performed using the GAUSSIAN03 package of programs,[54] using at the DFT level the default prune integration grid, which consists of 75 radial shells and 302 angular points per shell, resulting in about 7000 points per atom. Lacking the original numerical data, experimental (e, 2e) ionization cross sections were obtained by digitizing the experimental momentum distributions presented in refs 1−3 as a function of the target electron momentum, by means of the so-called "GetData Graph Digitizer" package.[55]

## III. Results and Discussion

**(a) Valence Electronic Structure and Ionization Spectra.** Inspection of Figure 2 and comparison of the ADC(3)/6-31G, ADC(3)/cc-pVDZ, and ADC(3)/DZP+ ionization spectra therein confirm readily the overall limited influence of the basis set upon relative ionization energies, including shake-up ionization energies, as well as on convoluted spectral envelopes, and this up to the vertical double ionization (VDI) threshold, which has been located at ∼24.4 eV according to benchmark calculations employed coupled cluster theory with single, double, and perturbative triple excitations [CCSD(T)][56] in conjunction with the cc-pVDZ basis set located at ∼24.4 eV. The reader is referred to Table 1 and Figure 3 for a detailed assignment of available photoelectron measurements.[6b,8] All bands and shoulders (I−XIV) that emerge in these measurements are in clear one-to-one correspondence with our simulations.

As usual (see, e.g., refs 22d−h), improving the basis set results merely in a redistribution of the shake-up ionization intensity over more and more satellites (Figure 2), but without qualitatively any significant change in the shape and orbital assignment of spectral bands (due to the drop of pole strengths below the retained threshold of 0.005, no line was recovered at the ADC(3)/cc-pVDZ and ADC(3)/DZP+ levels for the lowest ($1a_1$) orbital in the $C_{2s}$ region). The influence of the basis set strongly increases close to and beyond the VDI threshold, where the computed shake-up states must merely be regarded as approximations to series of diffuse (Rydberg-like) excited states of the cation converging to the continuum, and of shake-off

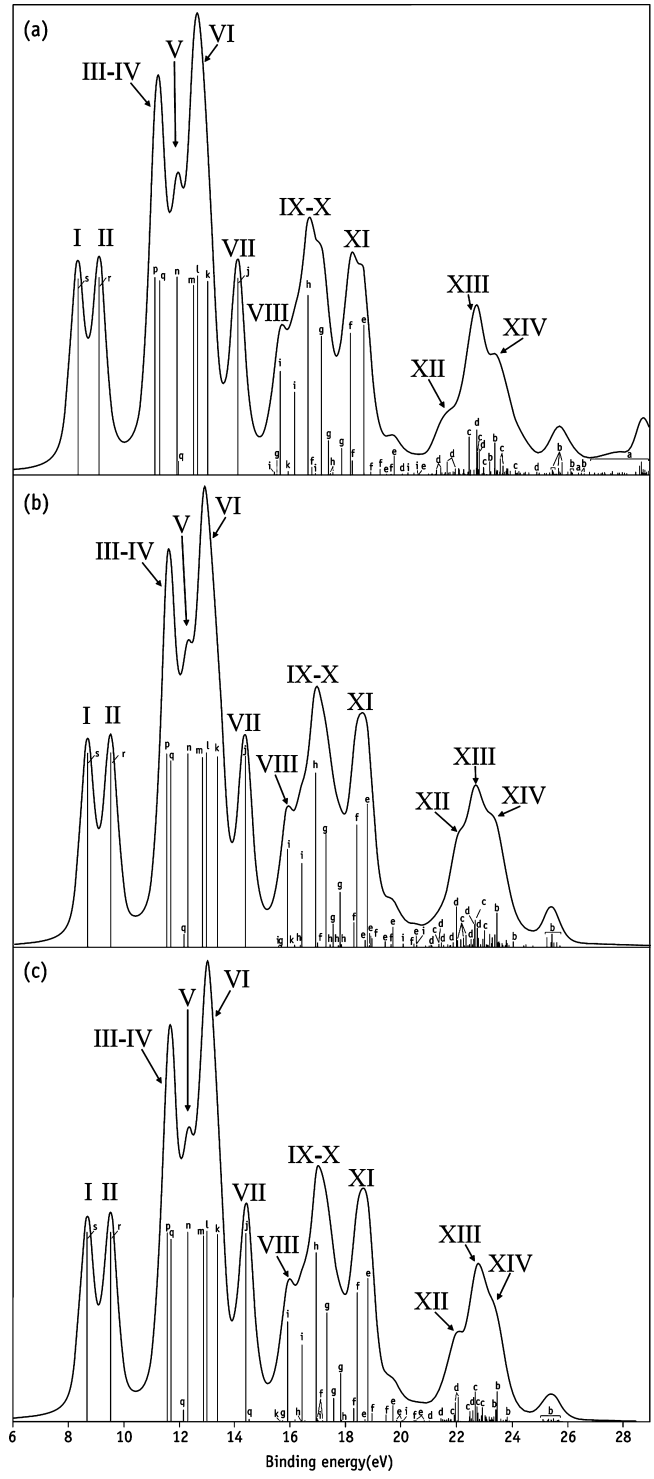


**Figure 2.** Theoretical ADC(3) ionization spectra of norbornadiene ($C_7H_8$, $C_{2v}$) obtained using the (a) 6-31G, (b) cc-pVDZ, and (c) Dunnig's DZP+ basis sets. See Tables 1 and 2 for a detailed orbital assignment of ionization lines (a−s) and a characterization of peaks I−XIV.

resonances embedded in the continuum. Although this conclusion may not be so fashionable nowadays, one may thus reaffirm the assertion that the 6-31G basis set is amply sufficient for reliably assigning the outer- and most inner-valence ionization bands of unsaturated hydrocarbons.[22d−j]

Further inspection of the ADC(3) and OVGF data reported in Tables 1 and 2 indicates in particular that sequential improvements of the basis set, from 6-31G to cc-pVDZ, and

**TABLE 1: ADC(3) Analyses of the Available Experimental (UPS and EMS) Ionization Spectra of Norbornadiene[a]**

| symbol | level | type | HF/ cc-pVDZ[b] | B3LYP/ cc-pVDZ[b] | ADC(3)/ 6-31G[b] | | ADC(3)/ cc-pVDZ[b] | | ADC(3)/ DZP+[b] | | He I[c,d] | He II[e] | EMS[f,g] |
|---|---|---|---|---|---|---|---|---|---|---|---|---|---|
| s | $5b_2$ | C−C ($\pi^-$) | 8.639 | 6.109 | 8.349 | (0.899) | 8.618 | (0.896) | 8.641 | (0.895) | 8.69 (I) | 8.41 (I) | 8.67 (A) |
| r | $7a_1$ | C−C ($\pi^+$) | 9.765 | 6.932 | 9.145 | (0.903) | 9.465 | (0.899) | 9.492 | (0.898) | 9.55 (II) | 9.24 (II) | 9.54 (B) |
| p | $2a_2$ | C−C ($\sigma$) | 12.450 | 8.879 | 11.155 | (0.904) | 11.481 | (0.894) | 11.541 | (0.892) | 11.26 (III) | 11.14 (III) | 11.40 (C) |
| | | | | | | | | | 14.497 | (0.014) | | | |
| q | $4b_1$ | C−C ($\sigma$) | 12.444 | 9.035 | 11.332 | (0.888) | 11.636 | (0.863) | 11.665 | (0.860) | ∼11.7 (IV) | ∼11.7 (IV) | 11.40 (C′) |
| | ($S_1$) | | | | 11.997 | (0.064) | 12.111 | (0.062) | 12.140 | (0.060) | | | |
| | | | | | | | | | 14.504 | (0.014) | | | |
| n | $4b_2$ | C−C ($\sigma$) | 13.264 | 9.438 | 11.950 | (0.907) | 12.242 | (0.898) | 12.290 | (0.896) | 12.51 (V) | 12.51 (V)[c,d] | 12.17 (D) |
| l | $6a_1$ | C−H ($\sigma$) | 14.114 | 10.015 | 12.690 | (0.910) | 12.910 | (0.900) | 12.981 | (0.898) | | | 12.77 (E) |
| m | $3b_1$ | C−C ($\sigma$) | 13.906 | 9.946 | 12.540 | (0.866) | 12.787 | (0.875) | 12.860 | (0.877) | ∼13.3 (VI) | ∼13.3 (VI)[c,d] | 13.25 (F) |
| k | $5a_1$ | C−H ($\sigma$) | 14.326 | 10.454 | 13.060 | (0.888) | 13.319 | (0.881) | 13.348 | (0.881) | | | 13.46 (G) |
| | | | | | 15.980 | (0.015) | 16.107 | (0.013) | 16.670 | (0.012) | | | |
| j | $3b_2$ | C−H ($\sigma$) | 15.688 | 11.284 | 14.160 | (0.899) | 14.324 | (0.888) | 14.381 | (0.887) | 14.24 (VII) | 13.89 (VII) | 14.26 (H) |
| i | $2b_2$ | C−H ($\sigma$) | 17.596 | 12.972 | 15.479 | (0.016) | 15.529 | (0.008) | 15.609 | (0.008) | | | |
| | | | | | 15.687 | (0.476) | 15.827 | (0.456) | 15.893 | (0.475) | 15.66 (VIII) | 15.62 (VIII) | 15.65 (I) |
| | ($S_2$) | | | | 16.208 | (0.379) | 16.359 | (0.388) | 16.413 | (0.368) | | | |
| | | | | | 16.953 | (0.006) | 16.928 | (0.011) | 17.007 | (0.011) | | | |
| | | | | | 20.302 | (0.014) | 20.018 | (0.016) | 20.058 | (0.006) | | | |
| | | | | | 20.673 | (0.007) | 20.505 | (0.010) | 20.165 | (0.005) | | | |
| | | | | | | | | | 20.529 | (0.006) | | | |
| h | $2b_1$ | C−H ($\sigma$) | 18.670 | 13.618 | 16.206 | (0.022) | 16.304 | (0.011) | 16.379 | (0.011) | | | |
| | | | | | 16.691 | (0.822) | 16.851 | (0.806) | 16.917 | (0.800) | 16.52 (IX) | 16.29 (IX) | 16.54 (J) |
| | | | | | 17.497 | (0.007) | 17.380 | (0.012) | 17.291 | (0.019) | | | |
| | | | | | 17.592 | (0.010) | 17.678 | (0.006) | 17.849 | (0.012) | | | |
| | | | | | | | 17.799 | (0.013) | | | | | |
| g | $4a_1$ | C−H ($\sigma$) | 19.052 | 14.137 | 15.566 | (0.005) | 15.619 | (0.006) | 15.699 | (0.006) | | | |
| | | | | | 17.170 | (0.635) | 17.241 | (0.523) | 17.302 | (0.528) | 17.16 (X) | 16.86 (X) | 17.05 (K) |
| | ($S_3$) | | | | 17.436 | (0.161) | 17.491 | (0.106) | 17.565 | (0.116) | | | 17.34 (L) |
| | ($S_4$) | | | | 17.902 | (0.124) | 17.743 | (0.253) | 17.809 | (0.236) | | | 17.91 (M) |
| | | | | | | | 21.632 | (0.009) | | | | | |
| f | $1a_2$ | C−H ($\sigma$) | 20.640 | 15.128 | 16.833 | (0.039) | 16.924 | (0.021) | 16.970 | (0.019) | | | |
| | | | | | 17.911 | (0.009) | 18.251 | (0.115) | 17.184 | (0.005) | | | |
| | | | | | 18.220 | (0.648) | 18.340 | (0.564) | 18.282 | (0.066) | | | |
| | | | | | 18.292 | (0.067) | 18.901 | (0.042) | 18.403 | (0.612) | ∼18.0 (XI) | 18.11 (XI) | 18.15 (N) |
| | | | | | 18.963 | (0.017) | 19.362 | (0.029) | 18.940 | (0.043) | | | |
| | | | | | 19.295 | (0.028) | 19.582 | (0.012) | 19.443 | (0.038) | | | |
| | | | | | 19.680 | (0.007) | 20.410 | (0.017) | 20.467 | (0.012) | | | |
| | | | | | 20.513 | (0.011) | | | | | | | |
| | | | | | 21.154 | (0.006) | | | | | | | |
| e | $3a_1$ | C−H ($\sigma$) | 20.995 | 15.317 | 18.703 | (0.685) | 18.643 | (0.035) | 18.692 | (0.015) | | | |
| | | | | | 19.519 | (0.005) | 18.724 | (0.657) | 18.773 | (0.679) | | | 18.54 (O) |
| | | | | | 19.795 | (0.089) | 18.807 | (0.007) | 19.692 | (0.081) | | | |
| | | | | | 20.698 | (0.009) | 19.643 | (0.095) | 19.833 | (0.009) | | | |
| | | | | | 21.276 | (0.005) | 20.498 | (0.010) | 20.044 | (0.008) | | | |
| | | | | | 22.351 | (0.007) | 21.060 | (0.007) | 20.533 | (0.011) | | | |
| | | | | | | | 22.237 | (0.005) | 20.825 | (0.009) | | | |
| d | $2a_1$ | C−C ($\sigma$) | 25.648 | 18.836 | 20.090 | (0.007) | 19.997 | (0.007) | 21.015 | (0.007) | | | |
| | | | | | 21.331 | (0.025) | 20.829 | (0.006) | 21.435 | (0.020) | | | |
| | | | | | 21.474 | (0.037) | 21.022 | (0.011) | 21.598 | (0.008) | | | |
| | | | | | 21.705 | (0.063) | 21.313 | (0.015) | 21.644 | (0.013) | | | |
| | | | | | 21.754 | (0.009) | 21.403 | (0.019) | 21.709 | (0.019) | | | |
| | | | | | 21.805 | (0.012) | 21.493 | (0.008) | 21.770 | (0.010) | | | |
| | | | | | 21.911 | (0.018) | 21.713 | (0.010) | 21.832 | (0.007) | | | |
| | | | | | 21.963 | (0.013) | 21.829 | (0.021) | 21.951 | (0.094) | | | |
| | | | | | 22.013 | (0.030) | 21.953 | (0.015) | 22.012 | (0.010) | | | |
| | | | | | 22.137 | (0.024) | 21.959 | (0.187) | 22.059 | (0.119) | | 21.5 (XII) | |
| | | | | | 22.289 | (0.008) | 22.109 | (0.035) | 22.411 | (0.006) | | | |
| | | | | | 22.439 | (0.006) | 22.468 | (0.036) | 22.468 | (0.028) | | | |
| | | | | | 22.500 | (0.014) | 22.553 | (0.030) | 22.493 | (0.006) | | | |
| | | | | | 22.545 | (0.025) | 22.589 | (0.022) | 22.581 | (0.057) | | | |
| | | | | | 22.667 | (0.026) | 22.607 | (0.110) | 22.583 | (0.009) | | | |
| | | | | | 22.769 | (0.211) | 22.698 | (0.090) | 22.676 | (0.025) | | | |
| | | | | | 22.857 | (0.120) | 22.824 | (0.010) | 22.732 | (0.037) | | | |
| | | | | | 23.037 | (0.008) | 22.887 | (0.017) | 22.741 | (0.023) | | | |
| | | | | | 23.125 | (0.007) | 23.015 | (0.013) | 22.769 | (0.046) | | | |
| | | | | | 23.259 | (0.006) | 23.217 | (0.020) | 22.818 | (0.017) | | | |
| | | | | | 23.609 | (0.010) | 23.577 | (0.020) | 22.918 | (0.028) | | | |
| | | | | | 23.725 | (0.008) | 23.618 | (0.009) | 23.018 | (0.007) | | | |
| | | | | | 23.886 | (0.032) | 23.714 | (0.007) | 23.059 | (0.027) | | | |
| | | | | | 23.967 | (0.021) | | | 23.090 | (0.015) | | | |

**TABLE 1: Continued**

| symbol | level | type | HF/ cc-pVDZ[b] | B3LYP/ cc-pVDZ[b] | ADC(3)/ 6-31G[b] | | ADC(3)/ cc-pVDZ[b] | | ADC(3)/ DZP+[b] | | He I[c,d] | He II[e] | EMS[f,g] |
|---|---|---|---|---|---|---|---|---|---|---|---|---|---|
| | | | | | 24.213 | (0.006) | | | 23.588 | (0.015) | | | |
| | | | | | 24.247 | (0.011) | | | | | | | |
| | | | | | 24.302 | (0.017) | | | | | | | |
| | | | | | 24.348 | (0.010) | | | | | | | |
| | | | | | 24.461 | (0.007) | | | | | | | |
| | | | | | 24.489 | (0.007) | | | | | | | |
| | | | | | 24.650 | (0.005) | | | | | | | |
| | | | | | 24.938 | (0.013) | | | | | | | |
| | | | | | 25.228 | (0.008) | | | | | | | |
| c | $1b_1$ | C−C ($\sigma$) | 26.020 | 19.187 | 21.188 | (0.006) | 21.064 | (0.006) | 21.206 | (0.005) | | | |
| | | | | | 21.322 | (0.012) | 21.307 | (0.016) | 21.397 | (0.006) | | | |
| | | | | | 21.519 | (0.014) | 21.719 | (0.008) | 21.558 | (0.013) | | | |
| | | | | | 21.620 | (0.006) | 21.990 | (0.030) | 21.919 | (0.036) | | | |
| | | | | | 22.125 | (0.031) | 22.113 | (0.031) | 22.051 | (0.009) | | | |
| | | | | | 22.174 | (0.005) | 22.201 | (0.041) | 22.121 | (0.006) | | | |
| | | | | | 22.306 | (0.027) | 22.299 | (0.055) | 22.476 | (0.051) | | | |
| | | | | | 22.460 | (0.017) | 22.371 | (0.008) | 22.525 | (0.019) | | | |
| | | | | | 22.502 | (0.176) | 22.457 | (0.012) | 22.671 | (0.146) | | 22.2 (XIII) | |
| | | | | | 22.550 | (0.006) | 22.527 | (0.006) | 22.727 | (0.074) | | | |
| | | | | | 22.748 | (0.030) | 22.557 | (0.037) | 22.762 | (0.016) | | | |
| | | | | | 22.794 | (0.089) | 22.619 | (0.127) | 22.818 | (0.005) | | | |
| | | | | | 22.826 | (0.026) | 22.719 | (0.044) | 22.881 | (0.033) | | | |
| | | | | | 22.975 | (0.010) | 22.819 | (0.011) | 22.923 | (0.071) | | | |
| | | | | | 23.022 | (0.039) | 23.039 | (0.009) | 23.029 | (0.033) | | | |
| | | | | | 23.027 | (0.006) | 23.089 | (0.005) | 23.072 | (0.011) | | | |
| | | | | | 23.253 | (0.019) | 23.136 | (0.062) | 23.167 | (0.005) | | | |
| | | | | | 23.395 | (0.033) | 23.241 | (0.046) | 23.211 | (0.005) | | | |
| | | | | | 23.460 | (0.025) | 23.509 | (0.018) | 23.212 | (0.013) | | | |
| | | | | | 23.498 | (0.015) | 23.437 | (0.024) | 23.237 | (0.010) | | | |
| | | | | | 23.532 | (0.021) | 23.731 | (0.032) | 23.258 | (0.024) | | | |
| | | | | | 23.724 | (0.043) | 23.768 | (0.012) | 23.300 | (0.014) | | | |
| | | | | | 23.827 | (0.020) | 22.959 | (0.079) | 23.342 | (0.028) | | | |
| | | | | | 23.864 | (0.031) | 23.842 | (0.010) | 23.674 | (0.011) | | | |
| | | | | | 24.176 | (0.021) | 24.438 | (0.013) | 23.749 | (0.014) | | | |
| | | | | | 24.483 | (0.006) | | | 23.797 | (0.013) | | | |
| | | | | | 24.524 | (0.012) | | | | | | | |
| | | | | | 24.650 | (0.010) | | | | | | | |
| b | $1b_2$ | C−C ($\sigma$) | 27.627 | 20.315 | 21.472 | (0.008) | 21.750 | (0.008) | 21.791 | (0.016) | | | |
| | | | | | 21.634 | (0.015) | 21.821 | (0.009) | 21.931 | (0.008) | | | |
| | | | | | 21.745 | (0.011) | 21.957 | (0.009) | 22.944 | (0.006) | | | |
| | | | | | 22.665 | (0.008) | 22.423 | (0.013) | 23.116 | (0.006) | | | |
| | | | | | 23.239 | (0.063) | 22.897 | (0.040) | 23.166 | (0.018) | | | |
| | | | | | 23.422 | (0.150) | 23.016 | (0.006) | 23.181 | (0.026) | | | |
| | | | | | 23.621 | (0.076) | 23.078 | (0.011) | 23.274 | (0.019) | | | |
| | | | | | 23.785 | (0.015) | 23.121 | (0.019) | 23.321 | (0.009) | | | |
| | | | | | 23.841 | (0.005) | 23.215 | (0.009) | 23.408 | (0.058) | | | |
| | | | | | 23.907 | (0.007) | 23.252 | (0.009) | 23.411 | (0.012) | | | |
| | | | | | 23.982 | (0.019) | 23.333 | (0.060) | 23.454 | (0.147) | | 23.2 (XIV) | |
| | | | | | 24.296 | (0.010) | 23.403 | (0.159) | 23.770 | (0.013) | | | |
| | | | | | 24.663 | (0.009) | 23.469 | (0.025) | 23.824 | (0.027) | | | |
| | | | | | 25.289 | (0.009) | 23.749 | (0.007) | 23.896 | (0.007) | | | |
| | | | | | 25.402 | (0.012) | 23.832 | (0.010) | 25.105 | (0.016) | | | |
| | | | | | 25.501 | (0.026) | 23.995 | (0.026) | 25.141 | (0.007) | | | |
| | | | | | 25.544 | (0.014) | 24.369 | (0.007) | 25.242 | (0.006) | | | |
| | | | | | 25.585 | (0.005) | 24.708 | (0.005) | 25.279 | (0.013) | | | |
| | | | | | 25.633 | (0.007) | 25.200 | (0.047) | 25.314 | (0.016) | | | |
| | | | | | 25.719 | (0.034) | 25.351 | (0.023) | 25.346 | (0.006) | | | |
| | | | | | 25.733 | (0.012) | 25.391 | (0.062) | 25.388 | (0.013) | | | |
| | | | | | 25.771 | (0.018) | 25.450 | (0.021) | 25.411 | (0.010) | | | |
| | | | | | 25.797 | (0.010) | 25.567 | (0.024) | 25.486 | (0.019) | | | |
| | | | | | 25.856 | (0.059) | 25.572 | (0.006) | 25.549 | (0.006) | | | |
| | | | | | 26.022 | (0.005) | 25.679 | (0.006) | 25.601 | (0.005) | | | |
| | | | | | 26.065 | (0.015) | | | 25.617 | (0.011) | | | |
| | | | | | 26.184 | (0.018) | | | 25.639 | (0.007) | | | |
| | | | | | 26.216 | (0.014) | | | 25.673 | (0.014) | | | |
| | | | | | 26.239 | (0.011) | | | | | | | |
| | | | | | 26.561 | (0.011) | | | | | | | |
| | | | | | 26.657 | (0.007) | | | | | | | |
| a | $1a_1$ | C−C ($\sigma$) | 32.193 | 24.109 | 25.645 | (0.006) | | | | | | | |
| | | | | | 26.455 | (0.007) | | | | | | | |

**TABLE 1: Continued**

| symbol | level | type | HF/ cc-pVDZ[b] | B3LYP/ cc-pVDZ[b] | ADC(3)/ 6-31G[b] | | ADC(3)/ cc-pVDZ[b] | ADC(3)/ DZP+[b] | He I[c,d] | He II[e] | EMS[f,g] |
|---|---|---|---|---|---|---|---|---|---|---|---|
| | | | | | 26.855 | (0.015) | | | | | |
| | | | | | 27.034 | (0.011) | | | | | |
| | | | | | 27.168 | (0.007) | | | | | |
| | | | | | 27.276 | (0.008) | | | | | |
| | | | | | 27.315 | (0.010) | | | | | |
| | | | | | 27.392 | (0.013) | | | | | |
| | | | | | 27.432 | (0.006) | | | | | |
| | | | | | 27.627 | (0.009) | | | | | |
| | | | | | 27.681 | (0.019) | | | | | |
| | | | | | 27.864 | (0.011) | | | | | |
| | | | | | 27.878 | (0.007) | | | | | |
| | | | | | 27.921 | (0.012) | | | | | |
| | | | | | 28.037 | (0.013) | | | | | |
| | | | | | 28.101 | (0.011) | | | | | |
| | | | | | 28.202 | (0.008) | | | | | |
| | | | | | 28.519 | (0.016) | | | | | |
| | | | | | 28.667 | (0.045) | | | | | |
| | | | | | 28.720 | (0.064) | | | | | |
| | | | | | 28.772 | (0.010) | | | | | |
| | | | | | 28.789 | (0.027) | | | | | |
| | | | | | 28.822 | (0.007) | | | | | |
| | | | | | 28.845 | (0.023) | | | | | |
| | | | | | 28.856 | (0.021) | | | | | |
| | | | | | 28.882 | (0.007) | | | | | |
| | | | | | 28.907 | (0.013) | | | | | |
| | | | | | 28.974 | (0.018) | | | | | |
| | | | | | 29.010 | (0.009) | | | | | |
| | | | | | 29.126 | (0.010) | | | | | |
| | | | | | 29.180 | (0.006) | | | | | |
| | | | | | 29.214 | (0.010) | | | | | |
| | | | | | 29.235 | (0.011) | | | | | |
| | | | | | 29.296 | (0.007) | | | | | |
| | | | | | 29.601 | (0.006) | | | | | |
| | | | | | 29.677 | (0.007) | | | | | |
| | | | | | 29.713 | (0.016) | | | | | |

[a] Binding energies are given in eV, along with the ADC(3) spectroscopic factors, which are given in parentheses. Compare with Figures 2 and 4 for band assignment. [b] B3LYP/TZVP geometry. [c] Reference 6b. [d] Reference 13. [e] Our estimation and assignment based on the He II spectrum in Bieri et al.[8] [f] Our estimation and assignment based on the EMS spectra in Mackenzie-Ross et al.[3] [g] See Figure 5.

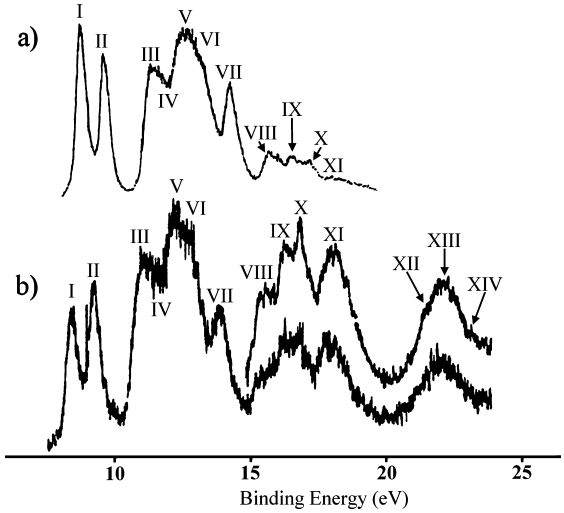


**Figure 3.** Experimental ionization spectra of norbornadiene ($C_7H_8$, $C_{2v}$) obtained using (a) He I and (b) He II. See Tables 1 and 2 for a characterization of peaks I−XIV.

then from cc-pVDZ to aug-cc-pVDZ or cc-pVTZ, result sequentially in rather uniform shifts, by ∼0.3 and ∼0.2 eV, respectively, of one-electron ionization lines toward lower binding energies. Except for the two outermost ionization lines, OVGF data obtained in conjunction with B3LYP/TZVP, B3LYP/cc-pVTZ, and MP2/aug-cc-pVDZ geometries indicate that one-electron ionization energies are not particularly sensitive to details of the computed molecular structures. Comparison of Tables 1 and 2 also confirms the now well-established rule[22f] that drops of OVGF pole strengths below a threshold value equal to 0.85 foretell a breakdown of the ionization spectrum at the ADC(3) level. A complete breakdown of the orbital picture of ionization is in particular observed at electron binding energies larger than 20 eV, where spectral bands are found to exclusively relate to highly intricate sets of shake-up lines.

The shake-up onset ($S_1$) is located at 12.1 eV. It corresponds to a rather intense satellite ($\Gamma = 0.06$) of the $4b_1$ orbital that relates dominantly to 2h-1p electronic configurations involving double electron removal from the $5b_2$ (HOMO) orbital and addition of an electron onto a $Xb_1$ orbital ($X = 6-12$). The most intense shake-up line of norbornadiene is the $S_2$ line at 16.4 eV ($\Gamma = 0.37$), which borrows its intensity from the main $2b_2^{-1}$ ionization line ($\Gamma = 0.47$) at 15.9 eV. Of relevance also for the analysis of (e, 2e) measurements in the sequel are two very intense satellites ($\Gamma > 0.10$) of the $4a_1^{-1}$ one-electron ionization line (g) at 17.3 eV, which emerge at binding energies around 17.6 and 17.8 eV (Table 1) and thus merely coincide with the minimum in the convoluted intensities (Figure 2) between bands X and XI. In the sequel, these two latter satellites will be further referred to as the $S_3$ and $S_4$ states. A more complete description

**TABLE 2: OVGF Analyses of the Available Experimental (UPS and EMS) Ionization Spectra of Norbornadiene[a]**

| symbol | level | OVGF/cc-pVDZ[b] | | OVGF/aug-cc-pVDZ[b] | | OVGF/cc-pVTZ[b] | OVGF/cc-pVDZ[c] | OVGF/cc-pVDZ[d] | He I[f,g] | He II[h] | EMS[i] |
|---|---|---|---|---|---|---|---|---|---|---|---|
| s | $5b_2$ | 8.501 | (0.905) | 8.643 | (0.902) | 8.696 (0.902) | 8.519 (0.905) | 8.359 (0.904) | 8.69 (I) | 8.41 (I) | 8.67 (A) |
| r | $7a_1$ | 9.364 | (0.907) | 9.517 | (0.904) | 9.437 (0.904) | 9.376 (0.907) | 9.269 (0.906) | 9.55 (II) | 9.24 (II) | 9.54 (B) |
| p | $2a_2$ | 11.307 | (0.903) | 11.465 | (0.900) | 11.401 (0.900) | 11.317 (0.904) | 11.393 (0.902) | 11.26 (III) | 11.14 (III) | 11.40 (C) |
| q | $4b_1$ | 11.529 | (0.908) | 11.667 | (0.905) | 11.584 (0.905) | 11.542 (0.908) | 11.524 (0.907) | ~11.7 (IV) | ~11.7 (IV) | 11.40 (C') |
| n | $4b_2$ | 12.136 | (0.906) | 12.299 | (0.903) | 12.236 (0.903) | 12.153 (0.906) | 12.100 (0.906) | 12.51 (V) | 12.51 (V)[f,g] | 12.17 (D) |
| l | $6a_1$ | 12.793 | (0.905) | 12.964 | (0.903) | 12.917 (0.902) | 12.803 (0.906) | 12.682 (0.904) | | | 12.77 (E) |
| m | $3b_1$ | 12.624 | (0.905) | 12.779 | (0.902) | 12.727 (0.902) | 12.633 (0.905) | 12.649 (0.906) | 13.3 (VI) | 13.3 (VI)[f,g] | 13.25 (F) |
| k | $5a_1$ | 13.199 | (0.899) | 13.345 | (0.896) | 13.254 (0.896) | 13.226 (0.899) | 13.107 (0.898) | | | 13.46 (G) |
| j | $3b_2$ | 14.206 | (0.900) | 14.375 | (0.897) | 14.304 (0.896) | 14.227 (0.900) | 14.058 (0.900) | 14.24 (VII) | 13.89 (VII) | 14.26 (H) |
| i | $2b_2$ | 15.863 | (0.874) | 15.963 | (0.869) | 15.954 (0.869) | 15.896 (0.874) | 15.777 (0.873) | 15.66 (VIII) | 15.62 (VIII) | 15.65 (I) |
| h | $2b_1$ | 16.797 | (0.878) | 16.884 | (0.874) | 16.906 (0.874) | 16.804 (0.878) | 16.753 (0.875) | 16.52 (IX) | 16.29 (IX) | 16.54 (J) |
| g | $4a_1$ | 17.233 | (0.876) | 17.336 | (0.872) | 17.325 (0.871) | 17.266 (0.876) | 17.123 (0.875) | 17.16 (X) | 16.86 (X) | 17.05 (K) |
| | | | | | | | | | | | 17.34 (L) |
| | | | | | | | | | | | 17.91 (M) |
| f | $1a_2$ | 18.280 | (0.834)[e] | | | 18.373 (0.828)[e] | 18.293 (0.835)[e] | 18.237 (0.823)[e] | ~18.0 (XI) | 18.11 (XI) | 18.15 (N) |
| e | $3a_1$ | 18.683 | (0.851) | 18.775 | (0.851) | 18.758 (0.845) | 18.704 (0.851) | 18.569 (0.849) | | | 18.54 (O) |

[a] Binding energies are given in eV, along with the OVGF spectroscopic factors, which are given in parentheses. [b] Based on B3LYP/TZVP. [c] Based on B3LYP/cc-pVTZ and. [d] Based on MP2/aug-cc-pVDZ geometry. [e] Breakdown of the MO picture of ionization; see ref 22f. [f] Reference 6b. [g] Reference 13. [h] Our estimation and assignment based on the He(II) Spectrum in Bieri et al.[8] [i] Our estimation and assignment based on the EMS Spectra in Mackenzie-Ross et al.[3]

**TABLE 3: Main Electronic Configurations Contributing to the Four Most Intense Shake-Up Lines[a]**

| shake-up line | ADC(3)/ 6-31G | ADC(3)/ cc-pVDZ | ADC(3)/ DZP+ |
|---|---|---|---|
| $S_1(4b_1)$ | $5b_2^{-2}5b_1^{+1}$ (0.064) | $5b_2^{-2}5b_1^{+1}$ (0.062) | $5b_2^{-2}7b_1^{+1}$ (0.060) |
| $S_2(2b_2)$ | $2a_2^{-1}5b_2^{-1}3a_2^{+1}$ (0.379) | $7a_1^{-1}2a_2^{-1}5b_1^{+1}$ (0.388) | $7a_1^{-1}2a_2^{-1}7b_1^{+1}$ (0.368) |
| $S_3(4a_1)$ | $7a_1^{-1}3b_1^{-1}5b_1^{+1}$ (0.161) | $7a_1^{-1}3b_1^{-1}5b_1^{+1}$ (0.106) | $7a_1^{-1}3b_1^{-1}7b_1^{+1}$ (0.116) |
| $S_4(4a_1)$ | $2a_2^{-1}5b_2^{-1}5b_1^{+1}$ (0.124) | $2a_2^{-1}5b_2^{-1}5b_1^{+1}$ (0.253) | $2a_2^{-1}5b_2^{-1}7b_1^{+1}$ (0.236) |

[a] Spectroscopic factors are given in parentheses.




**Figure 4.** Simulation of EMS spectra at azimuthal angles equal to $\phi = 0°$ (top) and $\phi = 10°$ (bottom) at an impact energy ($E_0$) equal to 1.5 keV plus the electron binding energy [ADC(3)/DZP + estimate], and using the following parameters: $\Delta\theta = 0.60°$, $\Delta\phi = 1.2°$, and FHWM = 0.9 eV.

of the most important electronic configurations to these four states is provided in Table 3.

The lower energy resolution obviously complicates the assignment of congested (e, 2e) ionization spectra. Prior to any analysis of (e, 2e) momentum distributions inferred from EMS experiments, it is always useful to identify from well-suited simulations employing ADC(3) ionization energies and the correspondingly calculated (e, 2e) ionization cross sections the sets of one-electron and shake-up ionized states that can be effectively resolved at various azimuthal angles ($\phi$). The reader is therefore now referred to Figures 4 and 5 for a comparison between such simulations at $\phi = 0$ and $\phi = 10°$ and the EMS ionization spectra at these angles by Mackenzie-Ross et al.,[2,3] along with the fitted Gaussians (A−N) that were obtained by deconvoluting these measurements up to an electron binding energy equal to 20 eV, by means of a least-squares fit procedure.[57] Note that the intricacy of shake-up bands (Figure 2) at larger binding energies rules out the possibility of carrying out any reliable experimental reconstruction of orbital momen-

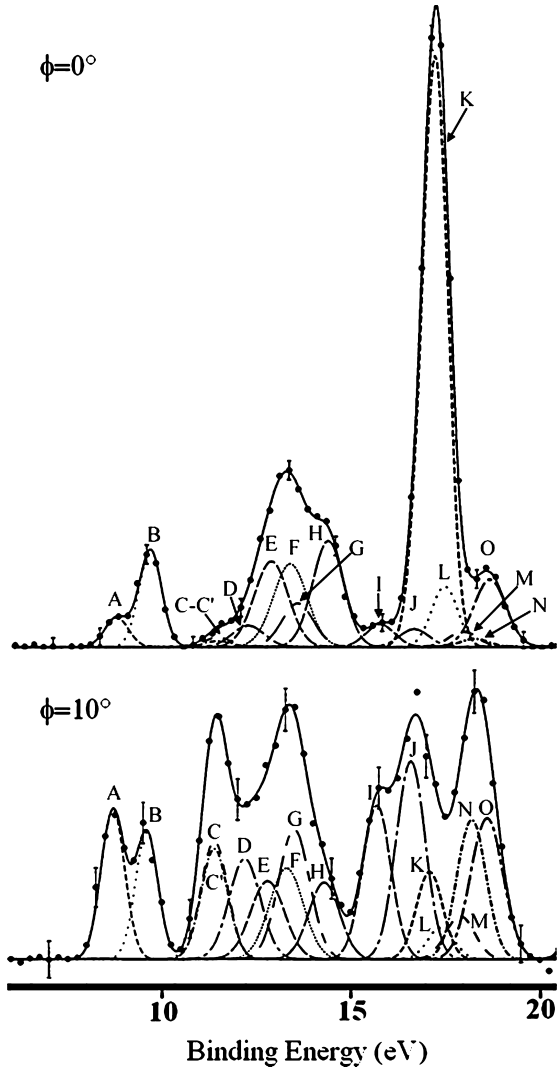


**Figure 5.** Experimental EMS results obtained at azimuthal angles equal to $\phi = 0°$ (top) and $\phi = 10°$ (bottom). Adapted from ref 3. See Tables 1 and 2 and text for a characterization and description of the Gaussian bands A−O.

tum distributions for the $2a_1$, $1b_1$, and $1b_2$ orbitals, through an accurate enough angular analysis of the corresponding (e, 2e) ionization intensities. Note also that two Gaussian bands (C, C′) with the same width and location (∼11.4 eV) and almost equal intensities were ascribed to the $2a_2^{-1}$ and $4b_1^{-1}$ one-electron ionization lines (Tables 1 and 2).

All our calculations definitely confirm that the $5b_2$ ($\pi^-$) orbital defines the ionization threshold of norbornadiene. Also, considering an energy separation of ∼0.85 eV compared with an energy resolution of ∼0.54 eV, our calculations confirm that the $5b_2$ ($\pi^-$) and $7a_1$ ($\pi^+$) orbitals are well resolved enough to afford individually an experimental reconstruction of their associated momentum profiles. On the other hand, whereas Mackenzie-Ross et al. identified six resolved bands (C−H) at binding energies between 10 and 15 eV,[2,3] the peaks and shoulders that emerge from our simulations and the energy separations between fitted Gaussian bands suggest that only four sets of one-electron and shake-up ionized states can be retained at the ADC(3) level for carrying the analysis of (e, 2e) ionization intensities, as follows: $\{C + C'\} \equiv \{2a_2^{-1} + 4b_1^{-1}\}$, $D \equiv \{4b_2^{-1} + S_1\}$, $\{E + F + G\} \equiv \{3b_1^{-1} + 6a_1^{-1} + 5a_1^{-1}\}$, and $H \equiv \{3b_2^{-1}\}$. We note in particular that, with energy separations smaller than the admitted experimental energy resolution (0.55 eV), bands E, F, and G too strongly overlap to allow meaningful individual angular analyses of the underlying intensities. All our calculations (Tables 1 and 2) locate for instance the $3b_1^{-1}$ ionization line at ∼0.12 to ∼0.17 eV below the $6a_1^{-1}$ ionization line, thus in a reversed energy order compared with that inferred from an analysis of Figures 3 and 10 in ref 3 and in the Supporting Information of ref 3. Similarly, whereas Mackenzie-Ross et al. identified seven resolved bands (I−O) at binding energies between 15 and 20 eV,[2,3] our simulations and data suggest to consider only three sets of ionized states and Gaussian bands for extracting some relevant enough information about electron momentum distributions at this binding energy range, as follows: $I \equiv \{2b_2^{-1} + S_2\}$; $\{J + K\} \equiv \{2b_1^{-1} + 4a_1^{-1} + S_3\}$, $\{N + O\} \equiv \{1a_2^{-1} + 3a_1^{-1}\}$. More precisely, momentum distributions inferred from the latter three sets of fitted Gaussians have been compared with simulations obtained by summing the contributions to momentum densities from ADC(3) Dyson orbitals related to all ionization lines located within the following energy intervals: (15.893−16.413 eV), (16.917−17.565 eV), and (18.282−19.692 eV), respectively.

Quite remarkably, while conducting the analysis, it appeared rather clearly that the Gaussian bands L and M that were empirically added at ∼17.3 and ∼17.9 eV in the deconvolution by Mackenzie-Ross et al. incidentally accounts for the presence at ∼17.6 and ∼17.8 eV of two rather intense satellites, $S_3$ ($\Gamma = 0.12$) and $S_4$ ($\Gamma = 0.24$). We note in particular that the angular dependence of the relative (e, 2e) ionization intensities recovered under these two bands rather closely follows (Figure 5) that of the most intense band K at ∼17.0 eV, an observation that confirms the relationships of these three bands with the $4a_1$ orbital: compared with bands I, J, N, and O, bands K, L, and M provide at $\phi = 0°$ leading contributions to (e, 2e) ionization intensities at binding energies between 15 and 20 eV, whereas these contributions are relatively much more limited at $\phi = 10°$. This seems to indicate an s-type momentum profile, in line with the symmetry characteristics of the $4a_1$ orbital.

Unfortunately, since the idea of a one-to-one correspondence between one-electron ionization lines and spectral bands was so strongly anchored in the work by Mackenzie-Ross et al.,[2,3] it appeared in our analysis that the contribution of the Gaussian bands L and M associated with the $S_3$ and $S_4$ lines were most probably discarded from their experimental reconstructions of the electron momentum profiles associated with the $2b_1^{-1} + 4a_1^{-1}$ and $1a_2^{-1} + 3a_1^{-1}$ sets of lines, which were ascribed to bands {J + K} and {N + O}, respectively. In the sequel, for the sake of scientific completeness and physical insight, we shall therefore compare simulations drawn with and without taking into account these two latter shake-up lines.

Except for the above restrictions on energy resolution and order, and on the role of shake-up lines, our assignment is overall very much in line with the assignment by Mackenzie-Ross et al.[2,3] of the ionization spectrum of norbornadiene at the He I binding energy range (0−21 eV). As shall be seen in the next section, the rescaling of momentum distributions they empirically proposed[2,3] for taking into account the flux of ionization intensities toward higher-lying shake-up and correlation bands appears also to be qualitatively consistent with our calculated ADC(3) pole strengths.

To terminate this section, we note that whereas HF/cc-pVDZ orbital energies provide rather reasonable estimates, by virtue of Koopmans' theorem, to the outermost experimental one-electron ionization energies (Table 1), B3LYP/cc-pVDZ Kohn−Sham orbital energies appear to severely underestimate the experiment, and this by several electronvolts. The inad-

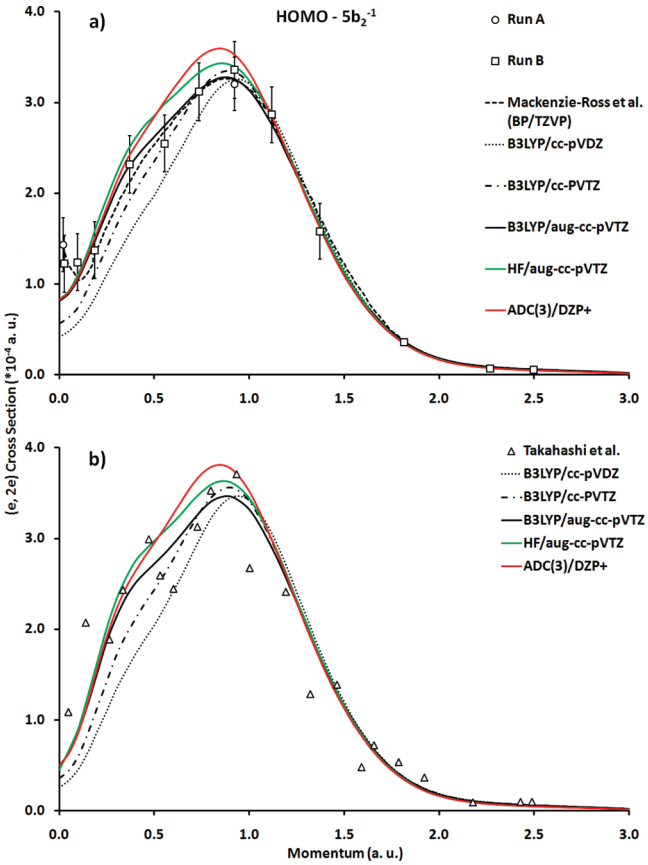


**Figure 6.** Comparison between experimental and theoretical electron momentum distributions for the HOMO using (a) $E_0 = 1.5$ keV, $\Delta\theta = 0.60°$, $\Delta\phi = 1.2°$ and (b) $E_0 = 0.8$ keV + 8.641 eV (binding energy), $\Delta\theta = 0.60°$, $\Delta\phi = 1.2°$. In (a) experimental results were taken from ref 2 along with the corresponding theoretical data presented in the same work at the BP/TZVP level by Mackenzie-Ross et al. In (b) experimental results are taken from the work by Takahashi et al.[1]

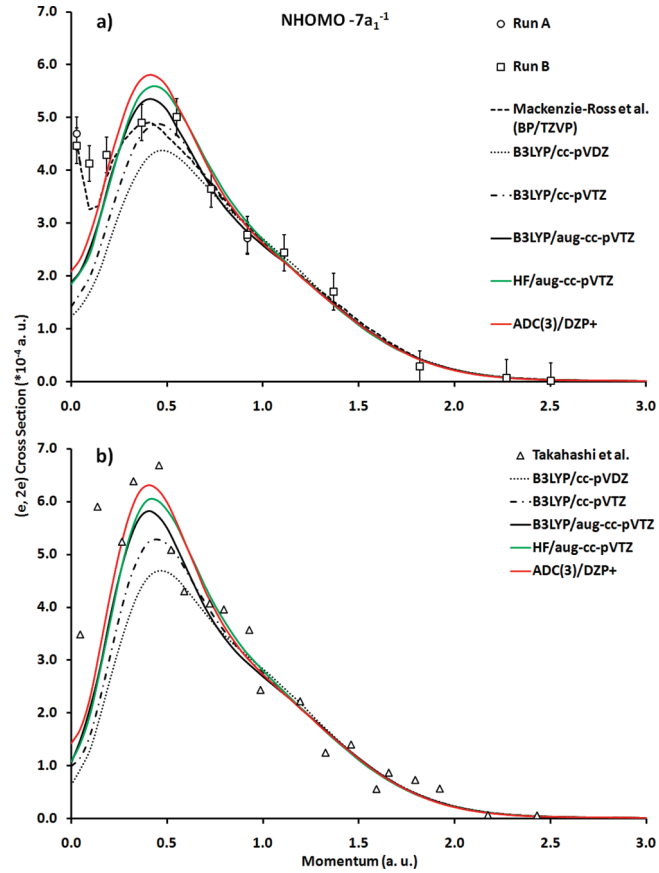


**Figure 7.** Comparison between experimental and theoretical electron momentum distributions for the NHOMO using (a) $E_0 = 1.5$ keV, $\Delta\theta = 0.60°$, $\Delta\phi = 1.2°$ and (b) $E_0 = 0.8$ keV + 9.492 eV (binding energy), $\Delta\theta = 0.60°$, $\Delta\phi = 1.2°$. In (a) experimental results were taken from ref 2 along with the corresponding theoretical data presented in the same work at the BP/TZVP level by Mackenzie-Ross et al. In (b) experimental results are taken from the work by Takahashi et al.[1]

equacy of the latter orbitals in reproducing the outermost experimental ionization energies reflects the sightedness of the employed exchange-correlation functional, and the too fast decay of the associated electronic potential in the asymptotic region (see ref 37 and references therein).

**(b) Electron Momentum Distributions.** The theoretical electron momentum distributions have been recast onto the relative intensity scales defined by the (e, 2e) experimental electron counts measured by Takahashi et al.[1] and Mackenzie-Ross et al.,[2,3] using in both cases rescaling factors obtained from a least-squares fit between experimental[2,3] and (interpolated) theoretical ADC(3)/DZP+ (e, 2e) ionization intensities for the two outermost ionization lines. The latter were computed at electron momenta ranging from 0.0 to 3.0 au in steps of 0.05 au. Considering the large fluxes in intensity toward larger electron binding energies that most orbitals undergo, these two lines are best suited for defining a common intensity scale, because of their large spectroscopic pole strengths ($\Gamma \sim 0.90$), their well-resolved nature, and the absence at nearby electron binding energies of any relevant shake-up state.

At the ADC(3) level, the dispersion of ionization intensity into shake-up processes is straightforwardly accounted for by the norm of Dyson orbitals. To also quantitatively account for the same effect, the (by definition normalized) Hartree−Fock and Kohn−Sham orbital momentum distributions that are provided in Figures 6−10 have been individually further rescaled using the correspondingly computed ADC(3)/DZP+ pole strengths (the contribution of shake-up lines is therefore also accounted for in the KS momentum distributions displayed in Figures 7 and 8).

All in all, it appears that HF, KS, and Dyson orbital distributions obtained in conjunction with the DZP+ or aug-cc-pVTZ basis sets provide essentially equivalent electron momentum profiles, and that overall quantitative agreement with experiment is amenable in all three cases, provided diffuse functions are included in the basis set. Since they were obtained using different electron impact energies, the results of Takahashi et al.[1] and Mackenzie-Ross et al.[2] for the HOMO and NHOMO have to be analyzed separately (Figures 6 and 7). All our results are perfectly consistent with both the experimental and theoretical (HF/6-31++G**) momentum distributions by Takahashi et al.[1] at $E_0 = 0.8$ keV (Figures 6b and 7b). In particular, the much lower electron count inferred for the HOMO at $p \rightarrow 0$ corroborates the symmetry characteristics of the $5b_2$ ($\pi^-$) orbital, which implies a p-type electron momentum profile (Figure 6b). Inversely, larger electron counts at $p \rightarrow 0$ are in line with the symmetry characteristics ($7a_1$) of the NHOMO ($\pi^+$), which strictly prevents a vanishing of resolution unfolded electron momentum distributions at $p \rightarrow 0$ (Figure 7b). Both for the HOMO (Figure 6b) and for the NHOMO (Figure 7b), all our simulations correctly predict a shoulder and maximum in the measured (e, 2e) intensities at $p \sim 0.5$ and $p \sim 0.9$ au, and at $p \sim 1.0$ and $p \sim 0.4$ au, respectively.

Very similar views prevail for our simulations of the momentum profiles inferred for these two orbitals (Figures 6a

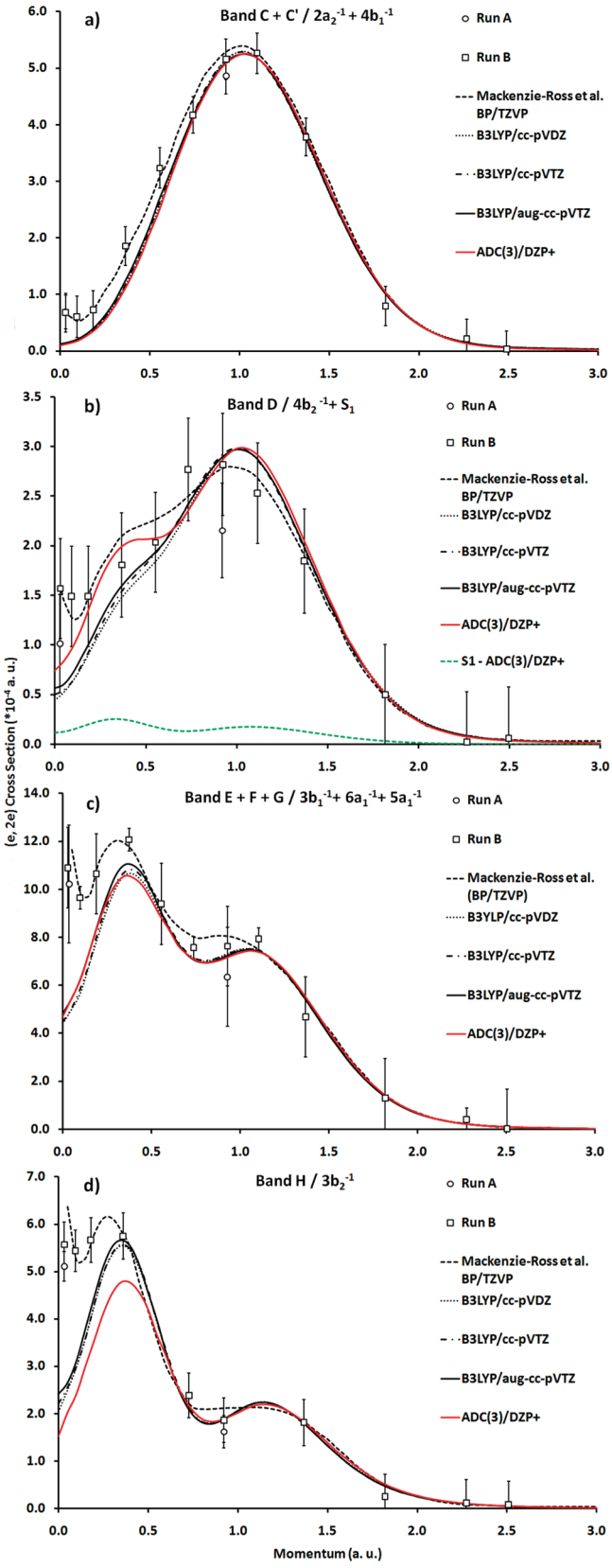


**Figure 8.** Comparison between experimental and theoretical momentum distributions for the following sets of Gaussian bands and ionization lines: (a) $\{C + C'\} \equiv \{2a_2^{-1} + 4b_1^{-1}\}$, (b) $D \equiv \{4b_2^{-1} + S_1\}$, (c) $\{E + F + G\} \equiv \{3b_1^{-1} + 6a_1^{-1} + 5a_1^{-1}\}$, and (d) $H \equiv \{3b_2^{-1}\}$; using the following parameters $E_0 = 1.5$ keV (+binding energy), $\Delta\theta = 0.60°$, $\Delta\phi = 1.2°$. Experimental results were taken from ref 3 along with the corresponding theoretical data presented in the same work at the BP/TZVP level by Mackenzie-Ross et al. In (b) we provide separately the (e, 2e) momentum profile produced by the $S_1$ state.

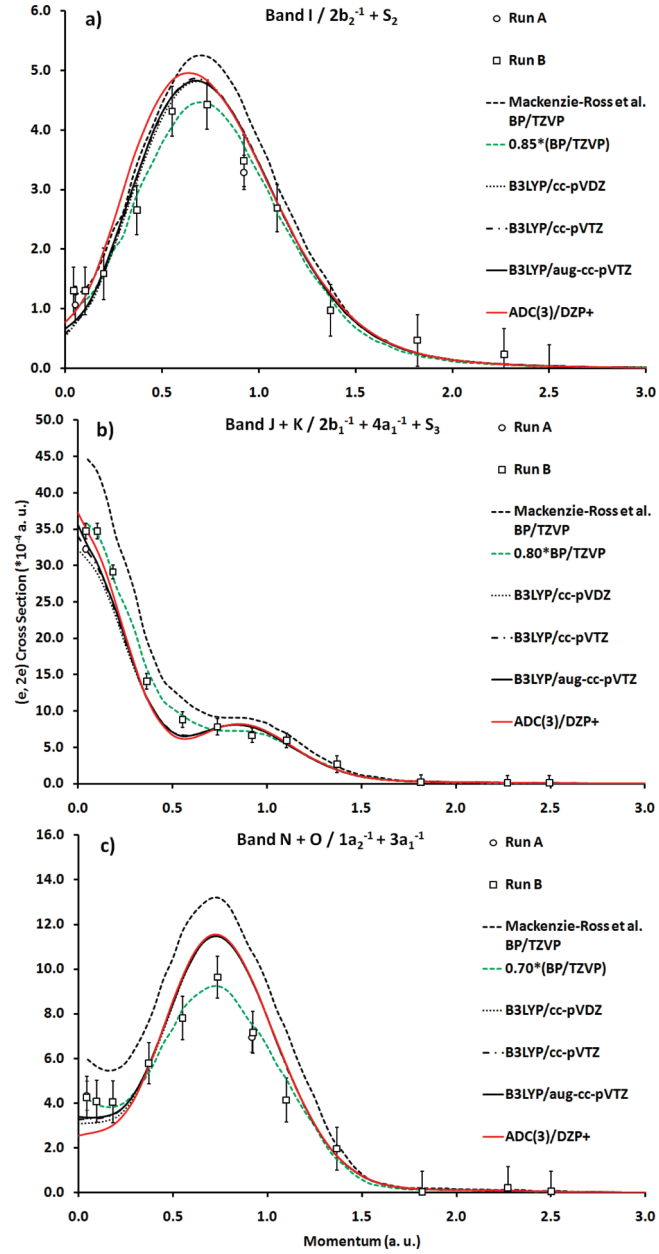


**Figure 9.** Comparison between experimental and theoretical momentum distributions for the following sets of Gaussian bands and ionization lines: (a) $I \equiv \{2b_2^{-1} + S_2\}$; (b) $\{J + K\} \equiv \{2b_1^{-1} + 4a_1^{-1} + S_3\}$, (c) $\{N + O\} \equiv \{1a_2^{-1} + 3a_1^{-1}\}$ using the following parameters $E_0 = 1.5$ keV (+binding energy), $\Delta\theta = 0.60°$, $\Delta\phi = 1.2°$. Experimental results were taken from ref 3 along with the corresponding theoretical data presented in the same work at the BP/TZVP level by Mackenzie-Ross et al.

and 7a) from the EMS measurements by Mackenzie-Ross et al. at $E_0 = 1.5$ keV (+binding energy),[2,3] except for one important but most annoying point. Whatever the level of theory employed, it appears indeed that many turns-ups of (e, 2e) ionization intensities at $p \rightarrow 0$ that were seen experimentally in the work by Mackenzie-Ross et al. and that were predicted therein on the ground of calculations employing the Becke−Perdew (BP) functional[58] in conjunction with Dunning's triple-$\zeta$ valence (TZVP) basis set[59] are not reproducible. Our HF, DFT, and ADC(3) calculations of momentum distributions demonstrates that electron correlation (or relaxation) effects *cannot* explain these turn-ups. Strangely enough, upon examining Figures 8−10, many similar problems are observed for most of the experimental (e, 2e) and theoretical (BP/TZVP) momen-

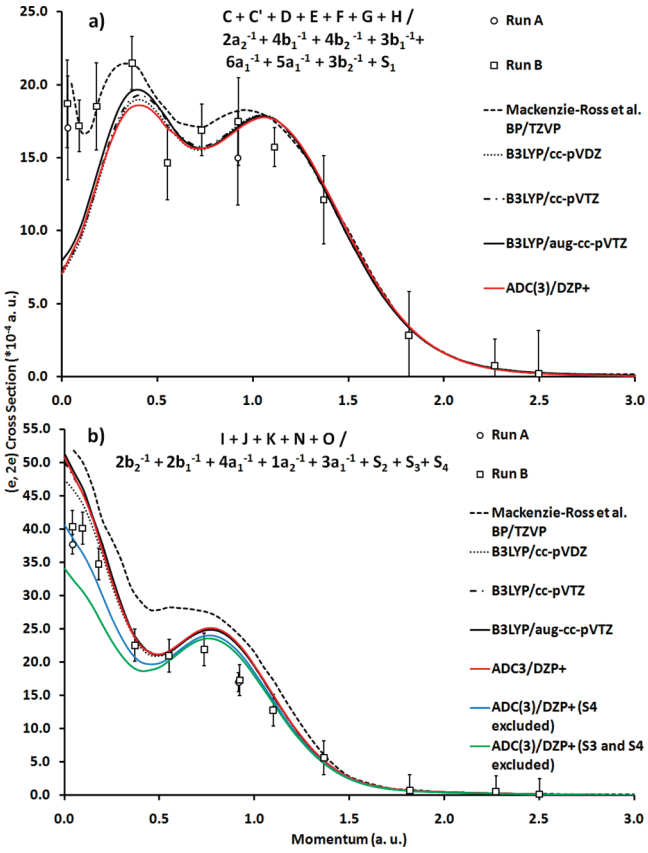


**Figure 10.** Comparison between experimental and theoretical momentum distributions for the following sets of Gaussian bands and ionization lines: (a) {C + C′ + D + E + F + G + H} and {I + J + K + N + O} using the following parameters: $E_0 = 1.5$ keV (+binding energy), $\Delta\theta = 0.60°$, $\Delta\phi = 1.2°$ as resolution folding. Experimental results were taken from ref 3 along with the corresponding theoretical data presented in the same work at the BP/TZVP level by Mackenzie-Ross et al. Our results include the contributions from *all* shake-up lines with pole strengths larger than 0.02 at binding energies (a) between 10 and 15 eV and (b) between 15 and 20 eV. In (b) we also provide separately the results of simulations excluding the $S_4$ satellite line, or excluding both the $S_3$ and $S_4$ lines.

tum densities inferred at low electron momenta by Mackenzie-Ross et al., which all our calculations seemingly underestimate.

The turn-ups observed by Mackenzie-Ross et al. for the HOMO and NHOMO at low electron momenta were tentatively ascribed to "electron correlation", apparently according to a comparison of calculations employing the so-called HF/GAUSSIAN and DFT/DGauss[60] packages of programs that were both interfaced to AMOLD.[4a] Since orbital topologies are strictly invariant to the retained level of theory, one may legitimately conclude that these turn-ups at $p \rightarrow 0$ in the computed BP/TZVP momentum profiles found their origin in some algorithmic problems with DGauss, or at least with its interface to AMOLD. Note that DGauss was itself part of Unichem, a now obsolete suite of computational quantum-chemistry programs written for (exceedingly fast) calculations on large pharmaceutical compounds, at the cost in DFT of a prune integration grid of much lower quality than with Gaussian, which by default consists of 1100 points only per atom.[60a] The BP/TZVP analysis which Mackenzie-Ross et al. made of the IR and Raman vibrational spectra of norbornadiene also indicates that geometry was optimized regardless of the $C_{2v}$ symmetry point group, considering that several calculated frequencies were left without any proper symmetry label, and that most formally IR-inactive $A_2$ modes were ascribed some intensity, regardless of dipole selection rules in IR spectroscopy (see Table 4 in ref 3 and compare it with the work by Jensen in ref 61 for an assignment of the vibrational spectra of norbornadiene upon a properly optimized $C_{2v}$ geometry). A lack of control upon the symmetry characteristics of orbitals combined with errors in numerical integrations at large values of $r$ may very well explain the too strong turn-ups and numerous oscillations that were theoretically predicted for several momentum profiles (Figure 8b−d) by Mackenzie-Ross et al. at low electron momenta ($p < 0.25$ au), apparently and strangely enough in excellent agreement with experiment.[2,3] In support of the assertion that many turn-ups at $p \rightarrow 0$ in the theoretical momentum distributions by Mackenzie-Ross et al. are numerical artifacts, note that, unlike DFT calculations, HF and ADC(3) calculations employing as here Gaussian-type AO basis sets are not subject to numerical integration problems, since all required one- and two-electron integrals are evaluated analytically.

Except for these discrepancies at very low electron momenta, our simulations based on the spectral assignment and intensity partitioning proposed in the preceding section are very much in line with the experimental (e, 2e) momentum distributions by Mackenzie-Ross et al.[2,3] In line with the symmetry characteristics of the contributing orbitals ($2a_2$, $4b_1$), band {C + C′} at ∼11.4 eV is characterized by a typical p-type profile, with one maximum at $p \sim 1.0$ au (Figure 8a). The presence of a shoulder at $p \sim 0.4$ au in the momentum profile experimentally inferred from band D at 12.2 eV and a comparison with our ADC(3) and B3LYP simulations (Figure 8b) seems to corroborate the presence of the shake-up line $S_1$ ($\Gamma = 0.06$) at 12.1 eV, which borrows its intensity to the $4b_1^{-1}$ one-electron ionization line at 11.4 eV. Notwithstanding the low momenta region, the combined experimental momentum distribution obtained by summing the contributions for bands E, F, and G at 12.77, 13.25, and 13.46 eV (Figure 8c) is all in all consistent with our calculations, which indicate two maxima at $p \sim 1.1$ au and $p \sim 0.4$ au, with an approximate intensity ratio of two-thirds and a minimum at $p \sim 0.8$ au. Similarly, according to all our simulations, and in fair agreement with the experimental momentum profile inferred from band H (Figure 8d), the individual $3b_2^{-1}$ one-electron ionization line produces a momentum distribution characterized by two maxima, at $p \sim 1.2$ au and at $p \sim 0.4$ au, this time exhibiting a one-third intensity ratio, again along with a minimum at $p \sim 0.8$ au.

Proceeding further (Figure 9), the interpretation of EMS experiments complicates tremendously, because the shake-up fragmentation of spectral bands intensifies with increasing ionization energy. These views are qualitatively consistent with the decreasing values of the rescaling factor, 0.85, 0.80, and 0.70, which Mackenzie-Ross et al. employed for improving the fit between their measurements and BP/TZVP calculations of momentum distributions inferred for the Gaussian bands I (Figure 9a), {J + K} (Figure 9b), and {N + O} (Figure 9c), respectively, to empirically account for the flux of ionization intensity toward shake-up and correlation bands at larger electron binding energies. In particular, and in line with the first of these three rescaling factors, the one-electron $2b_2^{-1}$ and $S_2$ shake-up lines at 15.9 and 16.4 eV yield a cumulative pole strength equal to 0.85 for the $2b_2$ ionization intensity flux, ascribed to band I at ∼15.7 eV. Considering that the outermost one-electron ionization lines were experimentally ascribed a spectroscopic pole strength equal to 1, compared with values around ∼0.90 at the ADC(3) level, the second rescaling factor (0.80) is also qualitatively in line with the ADC(3) pole strengths, ∼0.80 and ∼0.65 corresponding to the $2b_1^{-1}$ and $4a_1^{-1}$ ionization lines

ascribed to bands J and K (recalling that bands L and M were most probably not included in the analysis by MacKenzie-Ross et al.[2,3]). At last, the third rescaling factor appears to be rather close to the cumulative ADC(3) pole strengths, ~0.72 and ~0.67, which can be recovered for the $1a_2$ and $3a_1$ ionization intensities at the binding energy range corresponding to bands N + O.

In line with the symmetry characteristics of the related $2b_2$ orbital, band I exhibits experimentally and at all theoretical levels a typical p-type profile (Figure 9a). When any flux of $2b_2$ ionization intensity from band I to J is ignored, the complex of bands J + K produces one shallow minimum in (e, 2e) ionization intensity at $p \sim 0.5$ au, which is not seen on the experimental side (Figure 9b), probably as the result of too severe band overlaps and vibronic coupling complications. To investigate overlap effects, we consider in Figure 10a,b the global momentum profile experimentally inferred from bands {C + C′ + D + E + F + G + H} and {I + J + K + N + O} with electron momentum distributions obtained by summing the contributions of all one-electron and shake-up ionization lines at binding energies ranging from 10 to 15 eV, and from 15 to 20 eV, respectively. The agreement between our theoretical B3LYP and ADC(3) calculations and experiment is more than reasonable for the first set of bands (Figure 10a), at electron momenta larger than 0.25 au. For the second set (Figure 10b), it is clear that the (unrescaled) BP/TZVP data by Mackenzie-Ross et al.[3] strongly overestimate at all electron momenta the total (e, 2e) ionization intensities collected between 15 and 20 eV. With our ADC(3) data, it is also clear that the best agreement between theory and experiment is obtained when the contribution of the $S_4$ line is discarded. These two observations confirm our suggestion that the contributions of the Gaussian band M (and possibly L as well) were most probably not accounted for in the work by MacKenzie-Ross et al. Lacking their numerical data for *all* Gaussian bands (A−O), we cannot resolve this issue with certainty. Note nonetheless that the (e, 2e) ionization intensities recovered theoretically for the $1a_2$ and $3a_1$ orbitals under the {N + O} Gaussian band complex produce a p-type momentum profile (Figure 9c), in agreement with experiment, a conclusion implying again that band M ascribed in this work to the shake-up line $S_4$ originating from the $4a_1$ orbital was discarded from the analysis by Mackenzie-Ross et al. New EMS experiments on norbornadiene would be more than useful to assess quantitatively the role played by shake-up lines, in particular $S_2-S_4$.

## IV. Conclusions and Outlook for the Future

A thorough theoretical study of the electronic structure, ionization spectrum, and electron momentum distributions of norbornadiene has been presented, on the ground of 1p-GF/ADC(3) calculations of one-electron and shake-up ionization energies and of the related Dyson orbitals, and a comparison with available UPS and EMS experiments. Quantitative agreement is generally found between the UPS and EMS electron binding energies, on the one hand, and the results of large scale 1p-GF (OVGF, ADC(3)) calculations, on the other hand. These calculations and the comparison with results of independent EMS experiments[1−3] definitely confirm that norbornadiene is an unsaturated cage compound dominated by through-space interactions between $\pi$-bonds. With a shake-up onset ($S_1$) located at 12.1 eV ($\Gamma = 0.06$), numerous shake-up lines are found to tremendously complicate the analysis of the valence ionization bands and of the related momentum profiles. Where a comparison is possible, ADC(3) pole strengths are found to be qualitatively consistent with spectroscopic pole strengths determined from an empirical rescaling of DFT simulations against experimental (e, 2e) electron momentum distributions.[2,3] Besides $S_1$, spectroscopic fingerprints are somehow identifiable in the EMS experiments by MacKenzie-Ross et al.,[2,3] either from the shape of the momentum distributions or from extra Gaussian functions in their interpolation fit for three further intense shake-up lines ($S_2-S_4$) at ~16.4 eV ($\Gamma = 0.37$), ~17.6 eV ($\Gamma = 0.12$), and ~17.8 eV ($\Gamma = 0.24$). Particularly strong breakdowns of the one-electron picture of ionization at electron binding energies larger than 20 eV impede any reliable enough analysis of the experimental momentum distributions obtained at this binding energy range.

Comparison of HF, DFT (B3LYP), and ADC(3) Dyson orbital momentum distributions indicate that numerous turn-ups in (e, 2e) ionization intensities that were experimentally observed in the EMS experiments by Mackenzie-Ross et al.[2,3] *can certainly not* be due to electronic correlation (and relaxation). Most of these turn-ups may be due to an incorrect calibration of the absolute scale of azimuthal angles: all these turn-ups would indeed disappear if the reference $\phi = 0°$ was simply shifted by just 1°.[62] If all these turn-ups and numerous oscillations in (e, 2e) ionization intensities at low values of $p$ are not experimental artifacts, possible interpretations could reside in ultrafast nuclear motions induced by electron removals from a highly strained cage compound, combined with distorted wave and/or postcollision effects (note that since low values of $p$ correspond to large values of $r$, (e, 2e) intensities at $p \rightarrow 0$ should intrinsically correspond to ionization processes occurring on characteristic time scales much longer than the usually admitted values of ~0.01 to 0.1 fs,[63] which means that at low electron momenta the outcome of nuclear dynamical effects in the final state could become more clearly apparent).

Wave packet dynamical simulations and new EMS experiments on norbornadiene would be very much needed for sorting out these issues. Whereas our newly presented theoretical results are perfectly consistent with the results by Takahashi et al.,[1] we wish indeed to note that most of the calculations of momentum profiles using the Becke−Perdew (BP) exchange-correlation functional which Mackenzie-Ross et al. published in refs 2 and 3 are not reproducible at low momenta ($p < 0.25$ au), within the framework of the usual (first-order) Born, sudden, binary encounter and plane wave impulse approximations for interpreting EMS experiments.

**Acknowledgment.** All calculations presented in this work have been performed on Compaq ES45 and ES47 workstations at Hasselt University, Belgium. This work has been supported by the FWO-Vlaanderen, the Flemish branch of the Belgian National Science Foundation, and by the BijzonderOnderzoeks-Fonds (BOF: special research fund) at Hasselt University. F.M. acknowledges the "Bijzonder OnderzoeksFond" of Hasselt University for his Ph.D. fellowship. M.S.D. and B.H. also especially acknowledge financial support from a Research Program of the Research Foundation - Flanders (FWO_Vlaanderen; project number G.0350.09N, entitled "*From orbital imaging to quantum similarity in momentum space*"), and from the FWO research community "*Quantum chemistry: applied and fundamental aspects of Density Functional Theory*".

## References and Notes

(1) Takahashi, M.; Ogino, R.; Udagawa, Y. *Chem. Phys. Lett.* **1998**, *288*, 714.

(2) Mackenzie-Ross, H.; Brunger, M. J.; Wang, F.; Adcock, W.; Trout, N.; McCarthy, I. E.; Winkler, D. A. *J. Electron Spectrosc. Relat. Phenom.* **2002**, *123*, 389.

(3) Mackenzie-Ross, H.; Brunger, M. J.; Wang, F.; Adcock, W.; Maddern, T.; Campbell, L.; Newell, W. R.; McCarthy, I. E.; Weigold, E.; Appelbe, B.; Winkler, D. A. *J. Phys. Chem. A* **2002**, *106*, 9573.

(4) (a) McCarthy, I. E.; Weigold, E. *Rep. Prog. Phys.* **1991**, *91*, 789. (b) Coplan, M. A.; Moore, J. H.; Doering, J.-P. *Rev. Mod. Phys.* **1994**, *66*, 985. (c) Weigold, E.; McCarthy, I. E. *Electron Momentum Spectroscopy*; Kluwer Academic Plenum Publishers: New York, 1999.

(5) (a) Brion, C. E.; Cooper, G.; Zheng, Y.; Litvinvuk, I. V.; McCarthy, I. E.; Chem. Phys. 2001, *270*, 13 and references therein. (b) Neville, J. J.; Zheng, Y.; Brion, C. E. *J. Am. Chem. Soc.* **1996**, *118*, 10533. (c) Zheng, Y.; Neville, J. J.; Brion, C. E. *Science* **1995**, *270*, 5237. (d) Deleuze, M. S.; Wang, W. N.; Salam, A.; Shang, R. C. *J. Am. Chem. Soc.* **2001**, *123*, 4049. (e) Huang, Y. R.; Knippenberg, S.; Hajgató, B.; François, J.-P.; Deng, J. K.; Deleuze, M. S. *J. Phys. Chem. A* **2007**, *111*, 5879.

(6) (a) Bischof, P.; Hashmall, J. A.; Heilbronner, E.; Horning, V. *Helv. Chim. Acta* **1968**, *52*, 1745. (b) Bischof, P.; Hashmall, J. A.; Heilbronner, E.; Harnung, V. *Helv. Chim. Acta* **1969**, *52*, 1745.

(7) Demeo, D. A.; Yencha, A. J. *J. Chem. Phys.* **1970**, *53*, 4536.

(8) Bieri, G.; Burger, F.; Heilbronner, E.; Maier, J. P. *Helv. Chim. Acta* **1977**, *60*, 2213.

(9) Dewar, M. S. J.; Bodor, N.; Worley, S. D. *J. Am. Chem. Soc.* **1970**, *92*, 19.

(10) Palmer, M. H.; Findlay, R. H. *Chem. Phys. Lett.* **1972**, *15*, 416.

(11) Lindholm, Fridh, C.; Åsbrink, L. *Faraday Discuss. Chem. Soc* **1972**, *127*, 54.

(12) Heilbronner, E.; Schmelzer, A. *Helv. Chim. Acta* **1975**, *58*, 936.

(13) von Niessen, W.; Diercksen, G. H. F. *J. Electron Spectrosc. Relat. Phenom.* **1979**, *16*, 351.

(14) Castro, C. R.; Dutler, R.; Bauk, A.; Wieser, H. *J. Mol. Struct. (THEOCHEM)* **1987**, *152*, 241.

(15) Galasso, V. *Chem. Phys.* **1989**, *138*, 231.

(16) Paddon-Row, M. N.; Wong, S. S.; Jordan, K. D. *J. Am. Chem. Soc.* **1990**, *112*, 1710.

(17) Hoffmann, R.; Imamura, A.; Hehre, W. J. *J. Am. Chem. Soc.* **1968**, *90*, 1499.

(18) Hoffmann, R.; Heilbronner, E.; Gleiter, R. *J. Am. Chem. Soc.* **1970**, *92*, 706.

(19) Hoffmann, R. *Acc. Chem. Res.* **1971**, *4*, 1.

(20) Ohno, K.; Ishida, T.; Naitoh, Y.; Izumi, Y. *J. Am. Chem. Soc.* **1985**, *107*, 8082.

(21) Brion, C. E.; Cooper, G.; Feng, R.; Tixier, S.; Zheng, Y.; McCarthy, I. E.; Shi, Z.; Wolfe, S. In *Correlations, Polarization and Ionization in Atomic Systems*; Madison, D. H., Schulz, M.; Eds.; AIP Conference Proceeding No. 604; AIP: Melville, NY, 2002; pp 38−44.

(22) (a) Cederbaum, L. S.; Domcke, W.; Schirmer, J.; Von Niessen, W. *Adv. Chem. Phys.* **1986**, *65*, 115, and references therein. (b) Deleuze, M. S.; Cederbaum, L. S. *Adv. Quantum Chem.* **1999**, *35*, 77, and references therein. (c) Deleuze, M. S.; Giuffreda, M. G.; François, J.-P.; Cederbaum, L. S. *J. Chem. Phys.* **2000**, *112*, 5325. (d) Deleuze, M. S.; Trofimov, A. B.; Cederbaum, L. S. *J. Chem. Phys.* **2001**, *115*, 5859. (e) Deleuze, M. S.; Giuffreda, M. G.; François, J.-P. *J. Phys. Chem. A* **2002**, *106*, 5626. (f) Deleuze, M. S. *J. Chem. Phys.* **2002**, *116*, 7012. (g) Deleuze, M. S. *J. Phys. Chem. A* **2004**, *108*, 9244. (h) Kishimoto, N.; Hagihara, Y.; Ohno, K.; Knippenberg, S.; François, J.-P.; (i) Deleuze, M. S. *J. Phys. Chem. A* **2005**, *109*, 10535. (j) Deleuze, M. S. *Chem. Phys.* **2006**, *329*, 22. (k) Knippenberg, S.; Deleuze, M. S. *J. Electron Spectrosc. Relat. Phenom.* **2010**, *178−179*, 61.

(23) (a) Potts, A. W.; Edvardson, D.; Karlsson, L.; Holland, D. M. P.; MacDonald, M. A.; Hayes, M. A.; Maripuu, R.; Siegbahn, K.; von Niessen, W. *Chem. Phys.* **2000**, *254*, 385. (b) Trofimov, A. B.; Schirmer, J.; Holland, D. M. P.; Karlsson, L.; Maripuu, R.; Siegbahn, K.; Potts, A. W. *Chem. Phys.* **2001**, *263*, 167. (c) Potts, A. W.; Trofimov, A. B.; Schirmer, J.; Holland, D. M. P.; Karlsson, L. *Chem. Phys.* **2001**, *271*, 337. (d) Trofimov, A. B.; Schirmer, J.; Holland, D. M. P.; Potts, A. W.; Karlsson, L.; Maripuu, R.; Siegbahn, K. *J. Phys. B* **2002**, *35*, 5051. (e) Potts, A. W.; Holland, D. M. P.; Trofimov, A. B.; Schirmer, J.; Karlsson, L.; Siegbahn, K. *J. Phys. B: At. Mol. Opt. Phys.* **2003**, *36*, 3129. (f) Trofimov, A. B.; Schirmer, J.; Kobychev, V. B.; Potts, A. W.; Holland, D. M. P.; Karlsson, L. *J. Phys. B* **2006**, *39*, 305. (g) Powis, I.; Zaytseva, I. L.; Trofimov, A. B.; Schirmer, J.; Potts, A. W.; Holland, D. M. P.; Karlsson, L. *J. Phys. B* **2007**, *40*, 2019. (h) Holland, D. M. P.; Potts, A. W.; Karlsson, L.; Zaytseva, I. L.; Trofimov, A. B.; Schirmer, J. *Chem. Phys.* **2008**, *352*, 205. (i) Holland, D. M. P.; Potts, A. W.; Karlsson, L.; Zaytseva, I. L.; Trofimov, A. B.; Schirmer, J. *Chem. Phys.* **2008**, *353*, 47. (j) Trofimov, A. B.; Zaytseva, I. L.; Moskovskaya, T. E.; Vitkovskaya, N. M. *Chem. Heterocycl. Compd.* **2008**, *44*, 1101. (k) Zaytseva, I. L.; Trofimov, A. B.; Schirmer, J.; Plekan, O.; Feyer, V.; Richter, R.; Coreno, M.; Prince, K. C. *J. Phys. Chem. A* **2009**, *113*, 15142.

(24) (a) Pickup, B. T. *Chem. Phys.* **1977**, *19*, 193. (b) McWeeny, R.; Pickup, B. T. *Rep. Prog. Phys.* **1980**, *43*, 1065. (c) Deleuze, M.; Pickup, B. T.; Delhalle, J. *Mol. Phys.* **1994**, *83*, 655. (d) Seabra, G. M.; Kaplan, I. G.; Zakrzewski, V. G.; Ortiz, J. V. *J. Chem. Phys.* **2004**, *121*, 4142. (e) Oana, C. M.; Krylov, A. I. *J. Chem. Phys.* **2007**, *127*, 234106.

(25) (a) Schirmer, J.; Cederbaum, L. S.; Walter, O. *Phys. Rev. A* **1983**, *28*, 1237. (b) von Niessen, W.; Schirmer, J.; Cederbaum, L. S. *Comput. Phys. Rep.* **1984**, *1*, 57. (c) Schirmer, J.; Angonoa, G. *J. Chem. Phys.* **1989**, *91*, 1754. (d) Weikert, H.-G.; Meyer, H.-D.; Cederbaum, L. S.; Tarantelli, F. *J. Chem. Phys.* **1996**, *104*, 7122. (e) Deleuze, M. S.; Giuffreda, M. G.; François, J.-P.; Cederbaum, L. S. *J. Chem. Phys.* **1999**, *111*, 5851. (f) Deleuze, M. S. *Int. J. Quantum Chem.* **2003**, *93*, 191.

(26) (a) Pickup, B. T.; Goscinski, O. *Mol. Phys.* **1973**, *26*, 1013. (b) Cederbaum, L. S.; Hohlneicher, G.; von Niessen, W. *Mol. Phys.* **1973**, *26*, 1405. (c) Cederbaum, L. S.; Domcke, W. *Adv. Chem. Phys.* **1977**, *36*, 205. (d) von Niessen, W.; Schirmer, J.; Cederbaum, L. S. *Comput. Phys. Rep.* **1984**, *1*, 57. (e) Zakrewski, V. G.; von Niessen, W. *J. Comput. Chem.* **1993**, *14*, 13. (f) Ortiz, J. V. In *Computational Chemistry: Reviews of Current Trends*; Leszczynski, J., Ed.; World Scientific: Singapore, 1997; Vol. 2, p 1. (g) Linderberg, J.; Öhrn, Y. *Propagators in Quantum Chemistry*, 2nd ed.; Wiley-Interscience: New York, 2004.

(27) Knippenberg, S.; François, J.-P.; Deleuze, M. S. *J. Comput. Chem.* **2006**, *27*, 1703.

(28) (a) Deleuze, M. S. S.; Knippenberg, S. *J. Chem. Phys.* **2006**, *124*, 104309. (b) Huang, Y. R.; Hajgató, B.; Ning, C. G.; Zhang, S. F.; Liu, K.; Luo, Z. H.; Deng, J. K.; Deleuze, M. S. *J. Phys. Chem. A* **2008**, *112*, 2339. (c) Huang, Y. R.; Ning, C. G.; Deng, J. K.; Deleuze, M. S. *Phys. Chem. Chem. Phys.* **2008**, *10*, 2374.

(29) Deleuze, M. S.; Hajgató, B.; Morini, F.; Knippenberg, S. *J. Phys.: Conf. Series* **2010**, *212*, 012020.

(30) (a) Knippenberg, S.; Huang, Y. R.; Hajgató, B.; François, J.-P.; Deleuze, M. S. *J. Chem. Phys.* **2006**, *125*, 104309. (b) Xue, X. X.; Yan, M.; Wu., F.; Shan, X.; Xu., K. Z.; Chen, X. J. *Chin. J. Chem. Phys* **2008**, *21*, 515. (c) Yan, M.; Shan, X.; Wu., F.; Xia, X.; Wang, K. D.; Xu, K. Z.; Chen, X. J. *J. Phys. Chem. A* **2009**, *113*, 507. (d) Ning, C. G.; Luo, Z. H.; Huang, Y. R.; Hajgató, B.; Morini, F.; Liu, K.; Zhang, S. F.; Deng, J. K.; Deleuze, M. S. *J. Phys. B* **2008**, *41*, 175103. (e) Morini, F.; Hajgató, B.; Deleuze, M. S.; Ning, C. G.; Deng, J. K. *J. Phys. Chem. A* **2008**, *112*, 9083. (f) Morini, F.; Knippenberg, S.; Deleuze, M. S.; Hajgató, B. *J. Phys. Chem. A* **2010**, *114*, 4400.

(31) Hajgató, B.; Deleuze, M. S.; Morini, F. *J. Phys. Chem. A* **2009**, *113*, 7138.

(32) (a) Li, Z. J.; Chen, X. J.; Shan, X.; Liu, T.; Xu, K. Z. *J. Chem. Phys.* **2009**, *130*, 054302. (b) Wang, K. D.; Chen, L. Q.; Shan, X.; Wu, X. J.; Xu, K. Z.; Chen, X. J. *J. Electron. Spectrosc.* **2009**, *173*, 96. (d) Shan, X.; et al. *Chin. J. Chem. Phys.* **2009**, *22*, 642.

(33) (a) Brion, C. E.; Zheng, Y.; Rolke, J.; Neville, J. J.; McCarthy, I. E.; Wang, J. J. *J. Phys. B* **1998**, *31*, L223. (b) Takahashi, M.; Saito, T.; Hiraka, J.; Udagawa, Y. *J. Phys. B* **2003**, *36*, 2539. (c) Watanabe, N.; Takahashi, M.; Udagawa, Y.; Kouzakov, K. A.; Popov, Y. V. *Phys. Rev. A* **2007**, *75*, 052701.

(34) Parr, R. G.; Yang, W. *Density Functional Theory of Atoms and Molecules*; Oxford University Press: New York, 1989.

(35) (a) Becke, A. D. *J. Chem. Phys.* **1993**, *98*, 5648. (b) Lee, C.; Yang, W.; Parr, R. G. *Phys. Rev. B* **1988**, *37*, 785.

(36) Dunning, T. H., Jr. *J. Chem. Phys.* **1971**, *55*, 716.

(37) (a) Knippenberg, S.; Nixon, K. L.; Mackenzie-Ross, H.; Brunger, M. J.; Wang, F.; Deleuze, M. S.; François, J.-P.; Winkler, D. A. *J. Phys. Chem. A* **2005**, *109*, 9324. (b) Knippenberg, S.; Nixon, K. L.; Brunger, M. J.; Maddern, T.; Campbell, L.; Trout, N.; Wang, F.; Newell, W. R.; Deleuze, M. S.; François, J.-P.; Winkler, D. A. *J. Chem. Phys.* **2004**, *121*, 10525.

(38) Zheng, Y.; Pang, W. N.; Shang, R. C.; Chen, X. J.; Brion, C. E.; Ghanty, T. K.; Davidson, E. R. *J. Chem. Phys.* **1999**, *111*, 9526.

(39) Schmidt, M. W.; Baldridge, K. K.; Jensen, J. H.; Koseki, S.; Gordon, M. S.; Nguyen, K. A.; Windus, T. L.; Elbert, S. T. *QCPE Bull.* **1990**, *10*, 52.

(40) (a) Ruhe, A. *Math. Comput.* **1979**, *33*, 680. (b) Meyer, H.-D.; Pal, S. *J. Chem. Phys.* **1989**, *91*, 6195.

(41) (a) Liu, B. *Numerical Algorithms in Chemistry, Algebraic Methods*; LBL-8158; Lawrence Berkely Laboratory: Berkeley, CA. (b) Tarantelli, F.; Sgamellotti, A.; Cederbaum, L. S.; Schirmer, J. *J. Chem. Phys.* **1987**, *86*, 2201.

(42) Ning, C. G.; Liu, K.; Luo, Z. H.; Zhang, S. F.; Deng, J. K. *Chem. Phys. Lett.* **2009**, *476*, 157.

(43) Hehre, W. J.; Ditchfield, R.; Pople, J. A. *J. Chem. Phys.* **1972**, *56*, 2257.

(44) Dunning, T. H., Jr. *J. Chem. Phys.* **1989**, *90*, 1007.

(45) Dunning Jr., T. H.; Hay, P. J. In *Methods of Electronic Structure Theory*; Schaefer, H. F., Ed.; Plenum Press: New York, 1977; Vol. 2.

(46) Zheng, Y.; Brion, C. E.; Brunger, M. J.; Zhao, K.; Grisogono, A. M.; Braidwood, S.; Weigold, E.; Chakravorty, S. J.; Davidson, E. R.; Sgamellotti, A.; von Niessen, W. *Chem. Phys.* **1996**, *212*, 269.

(47) Duffy, P.; Chong, D. P.; Casida, M. E.; Salahub, D. R. *Phys. Rev. A* **1994**, *50*, 4707.

(48) Ning, C. G.; Ren, X. G.; Deng, J. K.; Su, G. L.; Zhang, S. F.; Knippenberg, S.; Deleuze, M. S. *Chem. Phys. Lett.* **2006**, *421*, 52. (b) Ning,

C. G.; Hajgató, B.; Huang, Y. R.; Zhang, S. F.; Liu, K.; Luo, Z. H.; Knippenberg, S.; Deng, J. K.; Deleuze, M. S. *Chem. Phys.* **2008**, *19*, 343.

(49) (a) Kendall, R. A.; Dunning, T. H.; Harrison, R. J. *J. Chem. Phys.* **1992**, *96*, 6796. (b) Woon, D. E.; Dunning, T. H. *J. Chem. Phys.* **1994**, *100*, 2975. (c) Peterson, K. A.; Woon, D. E.; Dunning, T. H. *J. Chem. Phys.* **1994**, *100*, 7410.

(50) See various contributions to the original HEMS program as recorded by Bawagan [A. O. Bawagan, Ph.D. Thesis, University of British Columbia (UBC), 1987]. The HEMS (now known as MOMAP) program has been extensively revised and extended at UBC by N. M. Cann and G. Cooper.

(51) Brunger, M. J.; Adcock, W. *J. Chem. Soc., Perkin Trans.* **2002**, *2*, 1.

(52) Bawagan, A. O.; Brion, C. E. *Chem. Phys.* **1990**, *144*, 167.

(53) Duffy, P.; Casida, M. E.; Brion, C. E.; Chong, D. P. *Chem. Phys.* **1992**, *159*, 347.

(54) Frisch, M. J.; et al. *GAUSSIAN03*, Revision D.01;Gaussian Inc., Pittsburgh, PA, 2003.

(55) See http://getdata-graph-digitizer.com/.

(56) (a) Purvis, G. D.; Bartlett, R. J. *J. Chem. Phys.* **1982**, *76*, 1910. (b) Scuseria, G. E.; Janssen, C. L.; Schaefer, H. F., III. *J. Chem. Phys.* **1988**, *89*, 7382. (c) Raghavachari, K.; Trucks, G. W.; Head-Gordon, M.; Pople, J. A. *Chem. Phys. Lett.* **1989**, *157*, 479. (d) Bartlett, R. J. *J. Phys. Chem.* **1989**, *93*, 1697. (e) Scuseria, G. E.; Lee, T. J. *J. Chem. Phys.* **1990**, *93*, 5851.

(57) Bevington, P. R.; Robinson, D. K. *Data Reduction and Error Analysis for the Physical Sciences*; McGraw-Hill Inc.: New York, 1990.

(58) (a) Becke, A. D. *Phys. Rev. A* **1988**, *38*, 3098. (b) Becke, A. D. *J. Chem. Phys.* **1988**, *88*, 2547. (c) Perdew, J. P. *Phys. Rev. B* **1986**, *33*, 8822.

(59) (a) Godbout, N.; Salahub, D. R.; Andzelm, J.; Wimmer, E. *Can. J. Chem.* **1992**, *70*, 560. (b) Sosa, C.; Andzelm, J.; Elkin, B. C.; Wimmer, E.; Dobbs, K. d.; Dixon, D. A. *J. Phys. Chem.* **1992**, *96*, 6630 (hese two references describe the TZVP basis set employed in DGauss).

(60) (a) Andzelm, J.; Wimmer, E. *J. Chem. Phys.* **1992**, *96*, 1290. (b) Komornicki, A.; Fitzgerald, G. J. *J. Chem. Phys.* **1993**, *98*, 1398.

(61) Jensen, J. O. *J. Mol. Struct. (THEOCHEM)* **2005**, *715*, 7.

(62) Suggestion by an anonymous referee.

(63) Such values are inferred by considering the time required by an electron with a kinetic energy of 1.5 keV to cover a distance of ∼3 to ∼30 Å, as rough estimates of molecular dimensions. See e.g.: Tobita, S.; Leach, S.; Jochims, H. W.; Rühl, E.; Illenberger, E.; Baumgärtel, H. *Can. J. Phys.* **2004**, *72*, 1060. These very crude estimates of the effective time scales of (e, 2e) ionization processes obviously neglect the wavelike properties of the target and emitted electrons, and of the long-range character of the Coulomb force.

JP105551J